EUROPEAN ORGANIZATION FOR NUCLEAR RESEARCH (CERN)

CMS-TOP-17-011

Measurement of the single top quark and antiquark production cross sections in the t channel and their ratio in proton-proton collisions at $\sqrt{s} = 13\,\text{TeV}$

The CMS Collaboration[*]

Abstract

Measurements of the cross sections for the production of single top quarks and antiquarks in the t channel, and their ratio, are presented for proton-proton collisions at a center-of-mass energy of 13 TeV. The data set used was recorded in 2016 by the CMS detector at the LHC and corresponds to an integrated luminosity of $35.9\,\text{fb}^{-1}$. Events with one muon or electron are selected, and different categories of jet and b jet multiplicity and multivariate discriminators are applied to separate the signal from the background. The cross sections for the t-channel production of single top quarks and antiquarks are measured to be $130 \pm 1\,\text{(stat)} \pm 19\,\text{(syst)}\,\text{pb}$ and $77 \pm 1\,\text{(stat)} \pm 12\,\text{(syst)}\,\text{pb}$, respectively, and their ratio is $1.68 \pm 0.02\,\text{(stat)} \pm 0.05\,\text{(syst)}$. The results are in agreement with the predictions from the standard model.

*See Appendix A for the list of collaboration members

1 Introduction

The study of single top quark production provides important insight into the electroweak processes of the standard model (SM) of elementary particles and into the structure of the proton. It also provides access to the magnitude of the Cabibbo–Kobayashi–Maskawa (CKM) matrix element V_{tb}. Among the production channels, the t-channel process is the dominant mechanism in proton-proton (pp) collisions at the CERN LHC accounting for approximately 70% of the total single top quark production cross section at $\sqrt{s} = 13$ TeV [1]. The t channel has a very distinct signature with a light quark, which is predominantly produced in the forward direction, and a top quark. Figure 1 illustrates the production of a single top quark and a single top antiquark. The flavor of the initial light quark defines the charge of the produced top quark; up quarks in the initial state result in top quarks, while down quarks produce top antiquarks. The ratio of the cross sections of these two processes provides insight into the inner structure of the proton as described by the parton distribution functions (PDFs). The ATLAS and CMS Collaborations have performed several measurements of the cross section for single top quark production in the t channel using LHC data collected at $\sqrt{s} = 7$, 8, and 13 TeV [2–9]. With a data set corresponding to an integrated luminosity of 35.9 fb^{-1}, the analysis described in this letter uses about 18 times more data compared to the previous analysis at 13 TeV [9] and also exploits the electron final state.
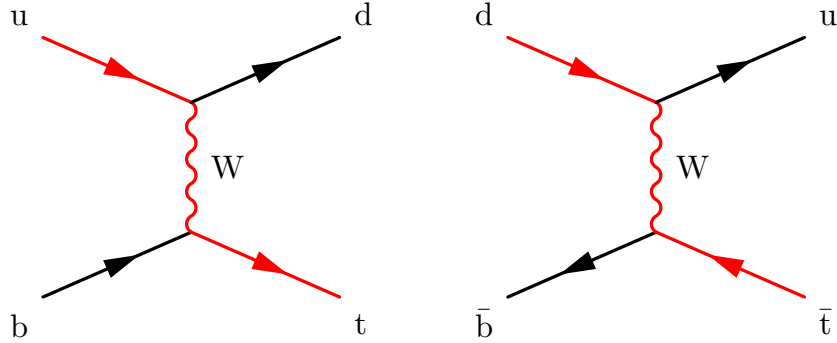

Figure 1: Feynman diagrams at Born level for the electroweak production of a single top quark (left) and antiquark (right). The flavor of the light quark in the initial state—either up quark (u) or down quark (d)—defines whether a top quark or top antiquark is produced.

The 13 TeV t-channel single top quark cross section has been calculated to next-to-leading-order (NLO) accuracy in quantum chromodynamics (QCD) using HATHOR 2.1 [10, 11]. Assuming a top quark mass of 172.5 GeV and $V_{tb} = 1$, the calculation yields cross section values of

$$\begin{aligned}
\sigma_{t\text{-ch},t} &= 136.0^{+4.1}_{-2.9}(\text{scale}) \pm 3.5(\text{PDF}+\alpha_S) \text{ pb,} \\
\sigma_{t\text{-ch},\bar{t}} &= 81.0^{+2.5}_{-1.7}(\text{scale}) \pm 3.2(\text{PDF}+\alpha_S) \text{ pb,} \\
\sigma_{t\text{-ch},t+\bar{t}} &= 217.0^{+6.6}_{-4.6}(\text{scale}) \pm 6.2(\text{PDF}+\alpha_S) \text{ pb,}
\end{aligned} \tag{1}$$

for the t-channel production of single top quarks ($\sigma_{t\text{-ch},t}$), single top antiquarks ($\sigma_{t\text{-ch},\bar{t}}$), and the sum of both subprocesses ($\sigma_{t\text{-ch},t+\bar{t}}$), respectively, where α_S is the strong coupling constant. The cross sections are evaluated in the five-flavor scheme (5FS), where the b quark is described by the PDF of the incoming protons. The quoted uncertainties are associated with the renormalization and factorization scales, as well as α_S at the mass of the Z boson, and PDFs. The PDF and $\alpha_S(m_Z)$ uncertainties were calculated with the MSTW2008 68% confidence level NLO [12, 13], CT10 NLO [14], and NNPDF2.3 [15] PDF sets, using the PDF4LHC prescription [16, 17]. A prediction at full next-to-next-to-leading-order (NNLO) accuracy [18] is also available for single

top quark production in the t channel at 13 TeV. As the available NNLO calculations consider only uncertainties from variations in the renormalization and factorization scales, the NLO prediction providing all required systematic uncertainty sources is used instead in this analysis for the normalization of the signal process. Depending on the PDF set used, the predicted values for the cross sections for the two processes and their ratio may differ, rendering the measurement sensitive to various PDF parameterizations. Using the cross section values and the PDF sets given above, the predicted value for the ratio $R_{t\text{-ch}} = \sigma_{t\text{-ch,t}}/\sigma_{t\text{-ch},\bar{t}}$ is 1.68 ± 0.08, where the uncertainty includes contributions due to variations of the renormalization and the factorization scales, the top quark mass, and the PDF and α_S.

The analysis uses events containing a single isolated muon or electron in the final state. The muon or electron originates from the decay of the W boson from the top quark decay, either directly or via $W \to \tau \nu$ and the following $\tau \to \ell \nu$ decay, where ℓ refers to either a muon or an electron. The main backgrounds come from the production of top quark-antiquark pairs ($t\bar{t}$) and from the production of W bosons in association with jets (W+jets). The separation between signal and background is achieved using boosted decision trees (BDTs), which combine the discriminating power of several kinematic distributions into a single classifier. The cross sections of t-channel single top quark and single top antiquark production, as well as the ratio of the two processes, are determined from a fit to the distributions of this single classifier.

2 The CMS detector

The central feature of the CMS apparatus is a superconducting solenoid of 6 m internal diameter, providing a magnetic field of 3.8 T. Within the solenoid volume are a silicon pixel and strip tracker, a lead tungstate crystal electromagnetic calorimeter (ECAL), and a brass and scintillator hadron calorimeter, each composed of a barrel and two endcap sections. Forward calorimeters extend the pseudorapidity (η) coverage provided by the barrel and endcap detectors. Muons are measured in the range $|\eta| < 2.4$, with detection planes made using three technologies: drift tubes, cathode strip chambers, and resistive plate chambers, embedded in the steel flux-return yoke outside the solenoid. The electron momentum is estimated by combining the energy measurement in the ECAL with the momentum measurement in the tracker. Events of interest are selected using a two-tiered trigger system [19]. The first level, composed of custom hardware processors, uses information from the calorimeters and muon detectors to select events. The second level, known as the high-level trigger, consists of a farm of processors running a version of the full event reconstruction software optimized for fast processing. A more detailed description of the CMS detector, together with a definition of the coordinate system used and the relevant kinematic variables, can be found in Ref. [20].

3 Simulation of events

Signal and background events are simulated to NLO accuracy with either the POWHEG or the MADGRAPH5_aMC@NLO [21] Monte Carlo (MC) event generator. The t-channel signal process [22] is simulated with POWHEG 2.0 [23–25] in the four-flavor scheme (4FS), where b quarks are produced via gluon splitting. This scheme yields a more precise description of the kinematic distributions of t-channel signal events than the 5FS [4, 26]. For the normalization of the signal samples the predictions derived in the 5FS (see Eq. (1)) are employed. The $t\bar{t}$ background [27] is simulated using POWHEG 2.0 and is normalized to the prediction calculated with TOP++ 2.0 [28]. The production of single top quarks associated to W bosons (tW) is simulated with POWHEG 1.0 in the 5FS [29], normalized to a prediction providing approxi-

mate NNLO accuracy [30, 31]. The value of the top quark mass in the simulated samples is $m_t = 172.5$ GeV. Events with W and Z bosons in association with jets are simulated using MADGRAPH5_aMC@NLO 2.2.2 and the FxFx merging scheme [32]. Predictions calculated with FEWZ 3.1 [33–35] are employed for the normalization of these two processes. For all samples, PYTHIA 8.212 [36] is used to simulate parton shower and hadronization. The underlying event is modeled for all samples using the tune CUETP8M1 [37], except for the $t\bar{t}$ sample, for which the tune CUETP8M2T4 [38] is used, which provides a more accurate description of the kinematic distributions of the top quark pair and of the jets in $t\bar{t}$ events. The parameterization of the PDFs used in all simulations is NNPDF3.0 NLO [39]. All of the generated events undergo a full simulation of the detector response using a model of the CMS detector implemented in GEANT4 [40]. Additional pp interactions within the same or nearby bunch crossing (pileup) are included in the simulation with the same distribution as observed in data.

4 Event selection and top quark reconstruction

In this analysis, the signature of the single top quark t-channel production process consists of a charged lepton, a neutrino, which is observed as p_T imbalance, a light-quark jet, which is often produced in the forward direction, and a jet arising from the hadronization of a bottom quark (b jet) from the top quark decay. A second b jet, arising in the production process via gluon splitting, generally has a softer p_T spectrum and a broader η distribution compared to the b jet originating from the top quark decay, and therefore often escapes detection. The event selection criteria are chosen according to this signature and events must contain one muon or electron candidate and at least two jets. Events in the muon channel are selected online using a trigger that requires an isolated muon with $p_T > 24$ GeV and $|\eta| < 2.4$. In the electron channel, a trigger is used that requires electrons with $p_T > 32$ GeV and $|\eta| < 2.1$. Only events for which at least one primary vertex is reconstructed are considered in the analysis. The primary vertex must be reconstructed from at least four tracks that have a longitudinal distance $|d_z| < 24$ cm and a radial distance $|d_{xy}| < 2$ cm from the interaction point. If more than one primary vertex is found in an event, the reconstructed vertex with the largest value of summed physics-object p_T^2 is taken to be the primary pp interaction vertex. The physics objects are the jets, clustered using the jet finding algorithm [41, 42] with the tracks assigned to the vertex as inputs, and the associated missing transverse momentum, taken as the negative vector sum of the p_T of those jets.

The particle-flow (PF) algorithm [43], which optimally combines information from all subdetectors, is used for the reconstruction of the individual particles. Muon candidates must have at least one hit in the muon detector and at least five hits in the silicon tracker. They are then reconstructed by a global fit to the information from the silicon tracker and the muon spectrometer. Selected muons must fulfill the criteria $p_T > 26$ GeV, $|\eta| < 2.4$, and relative isolation, $I_{rel} < 0.06$. The I_{rel} of a charged lepton candidate is calculated by summing the transverse energy deposited by photons and charged and neutral hadrons within a cone of size $\sqrt{(\Delta\eta)^2 + (\Delta\phi)^2} < 0.4$ (where ϕ is the azimuthal angle in radians) for muons and 0.3 for electrons around its direction, corrected for contributions from pileup [44], relative to its p_T.

Electron candidates are reconstructed by fitting tracks in the silicon tracker using the Gaussian-sum filter [45] and matching the tracks to energy clusters in the ECAL. The electron identification is performed using nine different variables and various selection criteria, including a requirement on the relative isolation $I_{rel} < 0.06$. Electrons are required to have $p_T > 35$ GeV and $|\eta| < 2.1$, while electrons falling in the gap between the ECAL barrel and endcap regions ($1.44 < |\eta| < 1.57$) are rejected. Events containing additional muons with $p_T > 10$ GeV and

$|\eta| < 2.4$ or additional electrons with $p_T > 15\,\text{GeV}$ and $|\eta| < 2.5$ are rejected. In both cases, the criteria on the lepton identification and isolation are relaxed ($I_{\text{rel}} < 0.2$ for muons; $I_{\text{rel}} < 0.18$ for electrons in the ECAL barrel and $I_{\text{rel}} < 0.16$ for electrons in the ECAL endcaps). Lepton p_T- and η-dependent scale factors are applied to correct for differences in the lepton reconstruction efficiencies between data and simulation.

Jets are clustered using the anti-k_T clustering algorithm [41] with a distance parameter of 0.4, as implemented in the FASTJET package [42]. The effect of additional tracks and calorimetric energy deposits from pileup on the jet momentum is mitigated by discarding tracks identified to be originating from pileup vertices and applying an offset correction to account for remaining contributions. Jet energy corrections are derived from simulation to bring the measured average response of jets to that of particle-level jets. In situ measurements of the momentum balance in dijet, γ+jet, Z+jet, and multijet events are used to account for any residual differences in the jet energy scale in data and simulation [46]. In this analysis, jets with $p_T > 40\,\text{GeV}$ and $|\eta| < 4.7$ are selected. The combined secondary vertex algorithm (CSVv2) [47] is used to identify b jets, which are required to have $p_T > 40\,\text{GeV}$ and $|\eta| < 2.4$. The efficiency to identify jets from b quarks is about 40% at the chosen working point, while the probability to misidentify jets from light quarks or gluons as b jets is 0.1%. Corrections to the simulation are applied in order to account for the difference in the b tagging efficiency in data and simulation.

To suppress the background from QCD multijet processes in the electron channel, events must fulfill $p_T^{\text{miss}} > 30\,\text{GeV}$. For events in the muon channel this variable is not sufficiently well modelled, and a requirement on the transverse mass of the W boson is imposed instead. The transverse mass of the W boson is defined as

$$m_T^W = \sqrt{\left(2 p_{T,\mu} p_T^{\text{miss}}\right)\left(1 - \cos\Delta\phi\right)} > 50\,\text{GeV}. \tag{2}$$

Here, p_T^{miss} is the magnitude of the transverse momentum vector $\vec{p}_T^{\text{miss}}$. This vector is defined as the projection onto the plane perpendicular to the beam axis of the negative vector sum of the momenta of all reconstructed PF objects in an event. The energy scale corrections applied to jets are propagated to $\vec{p}_T^{\text{miss}}$ [48]. The angle between the directions of the momentum vector of the muon and $\vec{p}_T^{\text{miss}}$ is $\Delta\phi$.

The selected events are divided into four different categories, depending on the number of selected jets and the number of b-tagged jets ($n$jets-$m$tags). The category with two selected jets, one of which is identified as originating from a bottom quark, i.e., 2jets-1tag category, provides the largest contribution of signal events constituting the signal category. Events with three selected jets with one or two of them b-tagged, namely events in the 3jets-1tag and 3jets-2tags categories, are dominated by $t\bar{t}$ production. These serve as control categories that are used in the fit to constrain the contribution from this dominant background process. Besides these categories, a fourth category containing events with two selected jets and no identified b jets, the 2jets-0tags category, is defined to validate the estimation of the QCD multijet background contribution in data.

The numbers of selected events are shown in Fig. 2 for the muon and electron channels. In both channels, the event yields are shown separately for events with positively and negatively charged muons (electrons). Positively charged leptons stem from top quarks and negatively charged leptons from top antiquarks. The contribution from the QCD multijet background is determined directly from data as described in Section 5. For the other processes, the event yields are derived from simulation.

The momentum four-vector of the top quark is reconstructed from the momenta of its decay
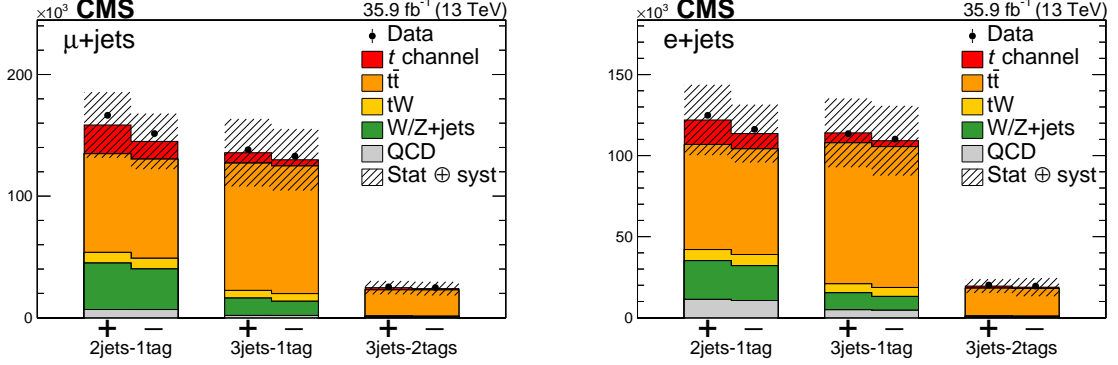
Figure 2: Event yields for the relevant processes in all categories after applying the full event selection in the muon (left) and electron (right) channels. The yields are shown separately for positively (+) and negatively (−) charged muons (electrons). The uncertainties include statistical and all systematic uncertainties. The yields are obtained from simulation, except for the QCD multijet contribution, which is derived from data (see Section 5).

products: the charged lepton, the reconstructed neutrino, and the b jet. The ambiguity of the assignment of one of the two b-tagged jets to the b quark from the top quark decay in the 3jets-2tags category is solved by choosing the b jet that leads to a reconstructed top quark mass closer to the top quark mass in the simulation. In the 3jets-1tag category, two untagged jets exist, of which the one with the highest $|\eta|$ is assigned to the light-quark jet in forward direction. The transverse momentum of the neutrino, $\vec{p}_{\mathrm{T},\nu}$, can be obtained from $\vec{p}_{\mathrm{T}}^{\mathrm{miss}}$. Assuming energy-momentum conservation at the $W\ell\nu$ vertex and setting the W boson mass to $m_{\mathrm{W}} = 80.4\,\mathrm{GeV}$, the longitudinal momentum of the neutrino, $p_{z,\nu}$, can be calculated as

$$p_{z,\nu} = \frac{\Lambda p_{z,\ell}}{p_{\mathrm{T},\ell}^2} \pm \frac{1}{p_{\mathrm{T},\ell}^2}\sqrt{\Lambda^2 p_{z,\ell}^2 - p_{\mathrm{T},\ell}^2(p_\ell^2 p_{\mathrm{T},\nu}^2 - \Lambda^2)}, \tag{3}$$

where

$$\Lambda = \frac{m_{\mathrm{W}}^2}{2} + \vec{p}_{\mathrm{T},\ell} \cdot \vec{p}_{\mathrm{T},\nu}, \tag{4}$$

and $p_\ell^2 = p_{\mathrm{T},\ell}^2 + p_{z,\ell}^2$ denotes the squared momentum of the charged lepton. In general, this procedure results in two possible solutions for $p_{z,\nu}$, which can have either real or complex values. If both solutions take real values, the one with the smallest absolute value is chosen [49, 50]. In the case of complex solutions, the transverse components of the neutrino momentum are modified such that the algebraic discriminant in Eq. (3) becomes null, while still fulfilling the constraint on the W boson mass. Of the possible solutions for $p_{x,\nu}$ and $p_{y,\nu}$ that resolve the problem of the negative discriminant, the coordinate pair that is closest to the corresponding components of $\vec{p}_{\mathrm{T}}^{\mathrm{miss}}$ is chosen.

5 Modeling and normalization of the QCD multijet background

Because of the theoretically challenging simulation of QCD multijet processes, this background contribution is suppressed as much as possible and the remaining contamination is modeled from data. As described in Section 4, requirements on $m_{\mathrm{T}}^{\mathrm{W}}$ or $p_{\mathrm{T}}^{\mathrm{miss}}$ are applied on the events in the muon and electron channels to suppress events from QCD multijet production. Different variables have been chosen for the two channels as $m_{\mathrm{T}}^{\mathrm{W}}$ is found to be better modeled compared to $p_{\mathrm{T}}^{\mathrm{miss}}$ in the muon channel and vice versa in the electron channel. These variables provide

the highest separation power between QCD multijet events and other processes, including the *t*-channel single top quark production, for the respective lepton final state. The remaining QCD contribution is modeled with samples of events derived from sideband regions in data enriched in QCD multijet events. These sideband regions are defined by inverting the muon or electron isolation requirements, while all other selection criteria described in Section 4 remain the same. As no reliable prediction for the QCD contribution to the selected data is available, the normalization for the QCD modeling samples are estimated from data. For that purpose, the same variables that are used to suppress this background contributions are explored by fitting their distributions over the entire range. A maximum likelihood fit is performed on the m_T^W or p_T^{miss} distribution using two probability density functions, one for the QCD multijet process and one for all other non-QCD processes. The latter distribution is obtained by adding the different non-QCD contributions from simulation, including the *t*-channel signal, according to their theory predictions, while the former is modeled using events from the sideband regions described above. The fit is performed separately in the 2jets-1tag and the 3jets-1tag categories. The contribution from QCD multijet events to the 3jets-2tags category is only minor and is neglected. To validate the QCD estimation procedure, this fit is also performed in the 2jets-0tags category, a signal-depleted category that provides a number of background events of this source larger by factors of 10 and 28 for the muon and electron channel, respectively. The entire range of the distributions is fitted and the resulting yields of the QCD multijet contribution are then used in the signal regions in which the requirements $m_T^W > 50\,\text{GeV}$ or $p_T^{miss} > 30\,\text{GeV}$ are applied. In this extrapolation, an uncertainty of 50% is applied to cover all effects from variations in the shape and rate of this background process. Figure 3 shows the fitted m_T^W and p_T^{miss} distributions in the 2jets-1tag, 3jets-1tag, and 2jets-0tags categories. Good agreement between the results of the fit and the data is found in the low-m_T^W and low-p_T^{miss} regions, where significant contributions from the QCD multijet background are expected. This simple two-template fit is designed to give a reliable estimate of the QCD multijet contribution and is not expected to describe also the tails of the fitted distributions with the same accuracy.

6   Signal extraction

BDT algorithms, implemented in the TMVA package [51] are employed to combine multiple variables into single discriminators, and thus enhance the separation between signal and background processes. Kinematic variables that are suitable to distinguish the single top quark *t*-channel signal process from the main background contributions are used for the BDT training. Each of these variables is required to be modeled reasonably in the simulation. The list of variables used for discrimination can be found in Table 1. The five most important variables are the light-quark jet $|\eta|$, the reconstructed top quark mass, which has high discrimination power against background processes where no top quarks are produced, the invariant mass of the dijet system consisting of the light-quark jet and the b-tagged jet from the top quark decay, the distance in the η–ϕ plane (ΔR) between the charged lepton and the b jet, and the cosine of the angle between the charged lepton and the light-quark jet in the rest frame of the top quark ($\cos\theta^*$). Figures 4 and 5 show the distributions of these five input variables from data compared to the simulation.

The BDTs are trained in the 2jets-1tag category, separately for muons and electrons. The lepton $|\eta|$ and m_T^W distributions are only considered in events with muons, while the p_T^{miss} variable is only used in the electron sample. The samples of simulated signal and background events, as well as the QCD multijet sample from sideband data, are normalized according to the respective predictions, with each sample split into two parts. One half is used for the training, while
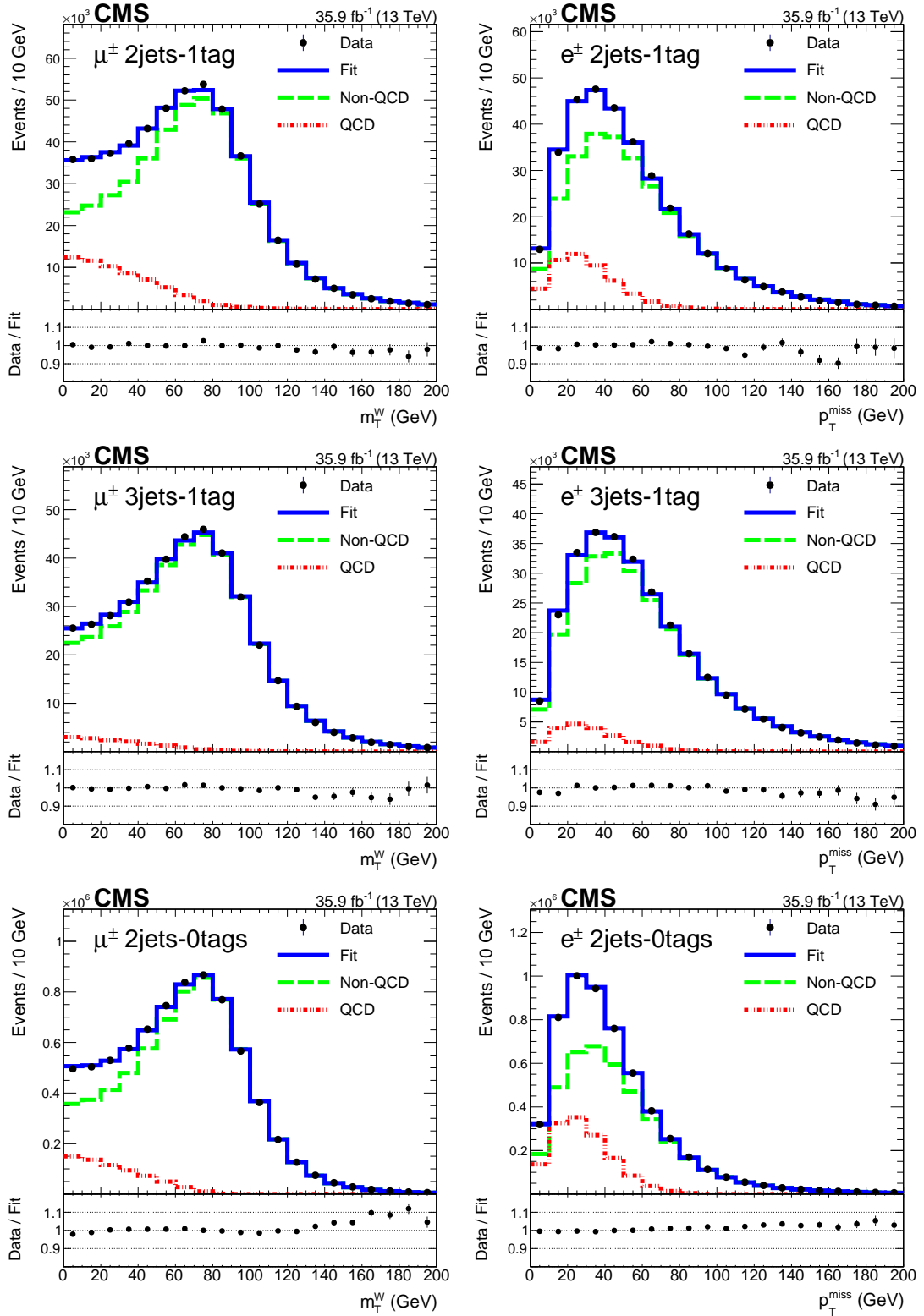
Figure 3: Outcome of the maximum likelihood fit to the m_T^W distribution of events with muons (left) and to the p_T^{miss} distribution for events with electrons (right) in the 2jets-1tag (upper row), 3jets-1tag (middle row), and the 2jets-0tags (lower row) categories. The QCD background template is extracted from the sideband region in data. For the fit, only statistical uncertainties are considered.

the other half serves for validation purposes and the actual measurement. The trained BDTs are then applied to the 2jets-1tag, 3jets-1tag, and 3jets-2tags categories, separately for the two different flavors and charges of the lepton.

A maximum likelihood fit is performed simultaneously on twelve different BDT output distributions (two lepton charges, two lepton flavors, three $n$jets-$m$tags categories). By including the categories with three selected jets in the fit, the $t\bar{t}$ background, which dominates these categories, is constrained. In this fit, the background rates are determined by introducing nuisance parameters, while the signal rate is a free parameter of the fit. The results of the fit are the cross sections for the production of single top quarks ($\sigma_{t\text{-ch},t}$) and antiquarks ($\sigma_{t\text{-ch},\bar{t}}$). The ratio of the two cross sections can be calculated from these two results propagating their uncertainties to the ratio using the covariance matrix of the fit. However, a more elegant and straightforward way of properly accounting for the correlations between the uncertainties in the two cross sections is used by repeating the fit with one of the two cross sections replaced by their ratio. This way, potential cancellations of uncertainties are taken into account directly in the fit and do not need to be calculated afterwards. The fitted distributions of the BDT output distributions are shown in Figs. 6 and 7. To verify the quality of the fit, for each distribution, the pull is also shown. The pull is defined as the difference between the distribution in data and the fitted one, divided by the uncertainty $\Delta = \sqrt{\Delta_{\text{data}}^2 - \Delta_{\text{fit}}^2}$, where Δ_{data} is the Poisson uncertainty in the data and Δ_{fit} is the uncertainty of the fit, including the statistical component and all uncertainties that have been included as nuisance parameters. As a cross-check, this fit is also performed separately for each lepton flavor. The obtained values are consistent within their uncertainties compared to the main results in the combined muon and electron channel.

7 Systematic uncertainties

Several sources of systematic uncertainties are considered in the analysis, either as nuisance parameters in the fit to the BDT distributions (profiled uncertainties) or as nonprofiled uncertainties. While most uncertainty sources, like purely experimental ones and uncertainties in the rates and the modeling of the backgrounds, can be profiled in the fit, this is not possible for those uncertainty sources that are related to the modeling of the signal process. As the results for the signal cross sections are given for the full phase space, the analysis contains an extrapolation from the phase space of the selected data set, in which the actual measurement takes place, to the full phase space, using predictions from the signal simulation about the shapes of the relevant distributions outside the measured area. Hence, the uncertainties in the modeling of the signal process apply not only to the phase space of the selected data set but to the full phase space and should therefore not get constrained from the fit in this reduced phase space. Their impact is determined by repeating the analysis using varied templates according to the systematic uncertainty sources under study in the fit instead of the nominal templates. The larger absolute shift in the parameter of interest, either caused by "down" or "up" variation of the systematic source under study, is taken as symmetric uncertainty in both directions. In the following, the different uncertainty sources that are considered in the analysis are briefly described. They are grouped in categories of related sources. It is indicated whether the uncertainty sources are implemented via shape morphing ("shape") or via normalization ("rate").

Nonprofiled uncertainties

- *Signal modeling (shape):* The following uncertainty sources cover potential mismodeling of the single top quark t-channel signal process. They are not considered as nuisance parameters in the fit but evaluated by repeating the full analysis using sam-
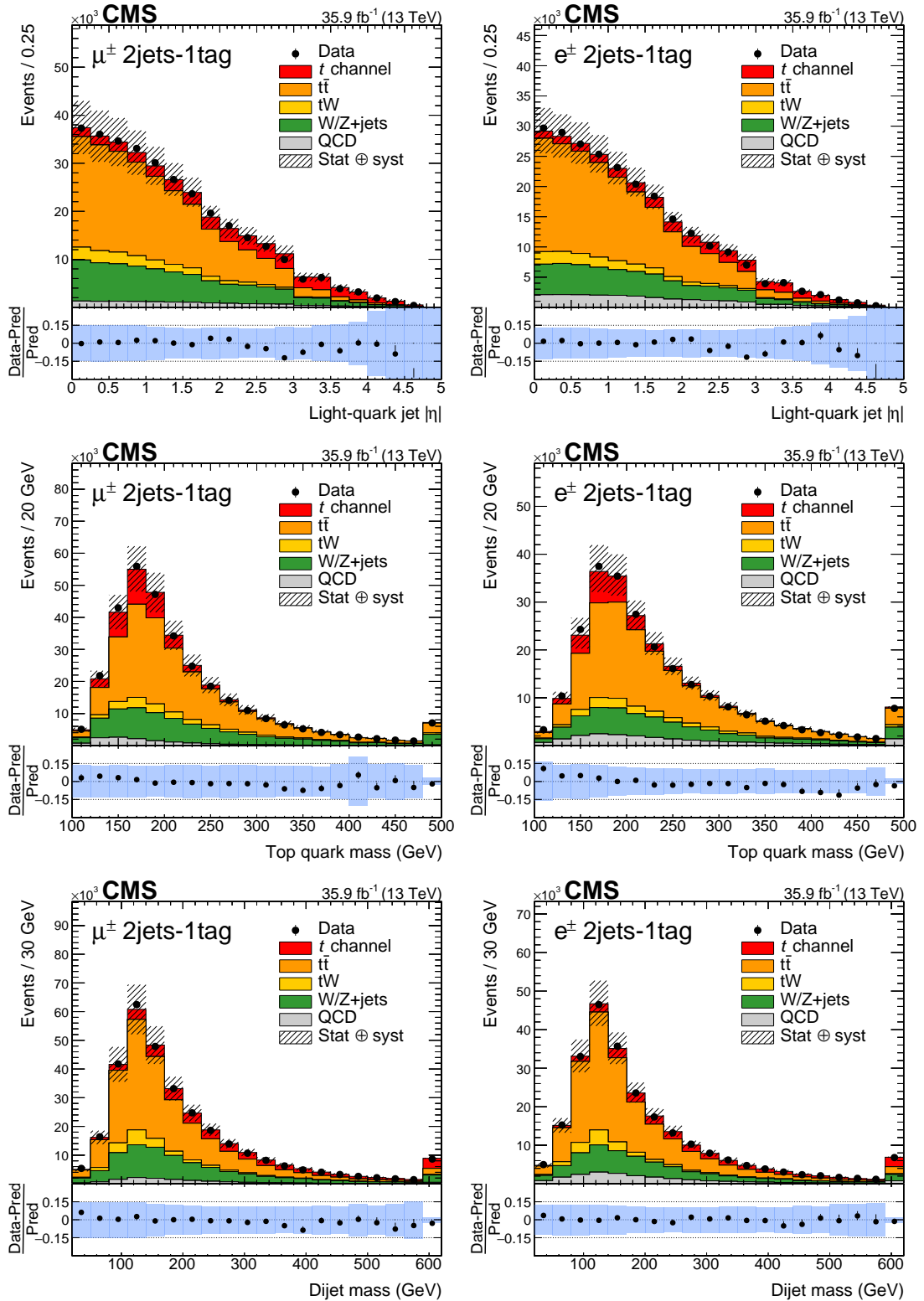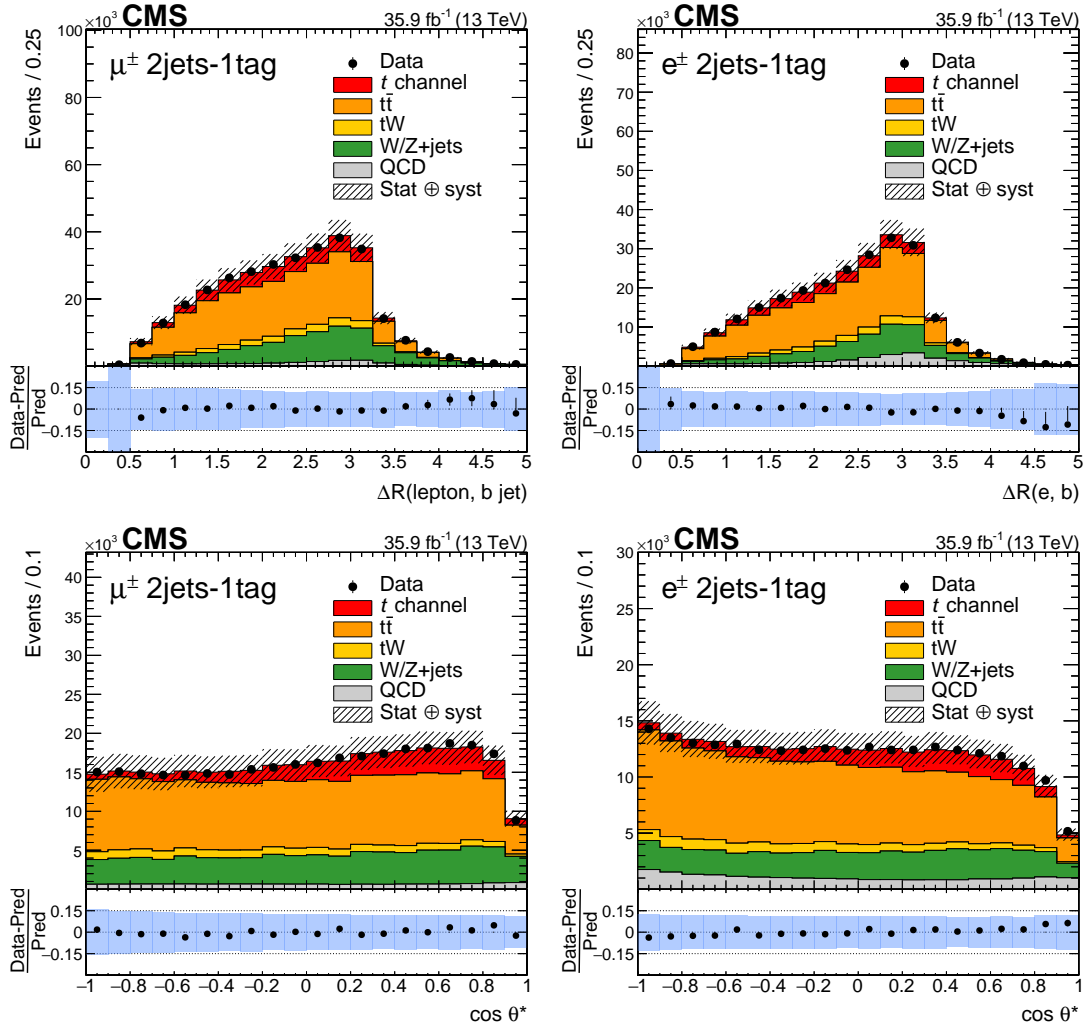
Figure 4: The three most discriminating input variables for the training of the BDTs in the muon channel (left) and in the electron channel (right): the absolute value of the pseudorapidity of the light-quark jet, the mass of the reconstructed top quark, the mass of the light-quark jet and the b-tagged jet associated to the top quark decay. The variables are ordered by their importance. The simulation is normalized to the total number of events in data. The shaded ares correspond to the quadratic sum of statistical and systematic uncertainties in the simulation before performing the fit. Also shown is the relative difference between the distributions in data and simulation in the lower panels.

Figure 5: The fourth and fifth most discriminating input variables for the training of the BDTs in the muon channel (left) and in the electron channel (right): the ΔR between the momentum vectors of the lepton and the b-tagged jet associated with the top quark decay, the cosine of the angle between the lepton and the light-quark jet in the rest frame of the top quark. The simulation is normalized to the total number of events in data. The shaded ares correspond to the quadratic sum of statistical and systematic uncertainties in the simulation before performing the fit. Also shown is the relative difference between the distributions in data and simulation in the lower panels.
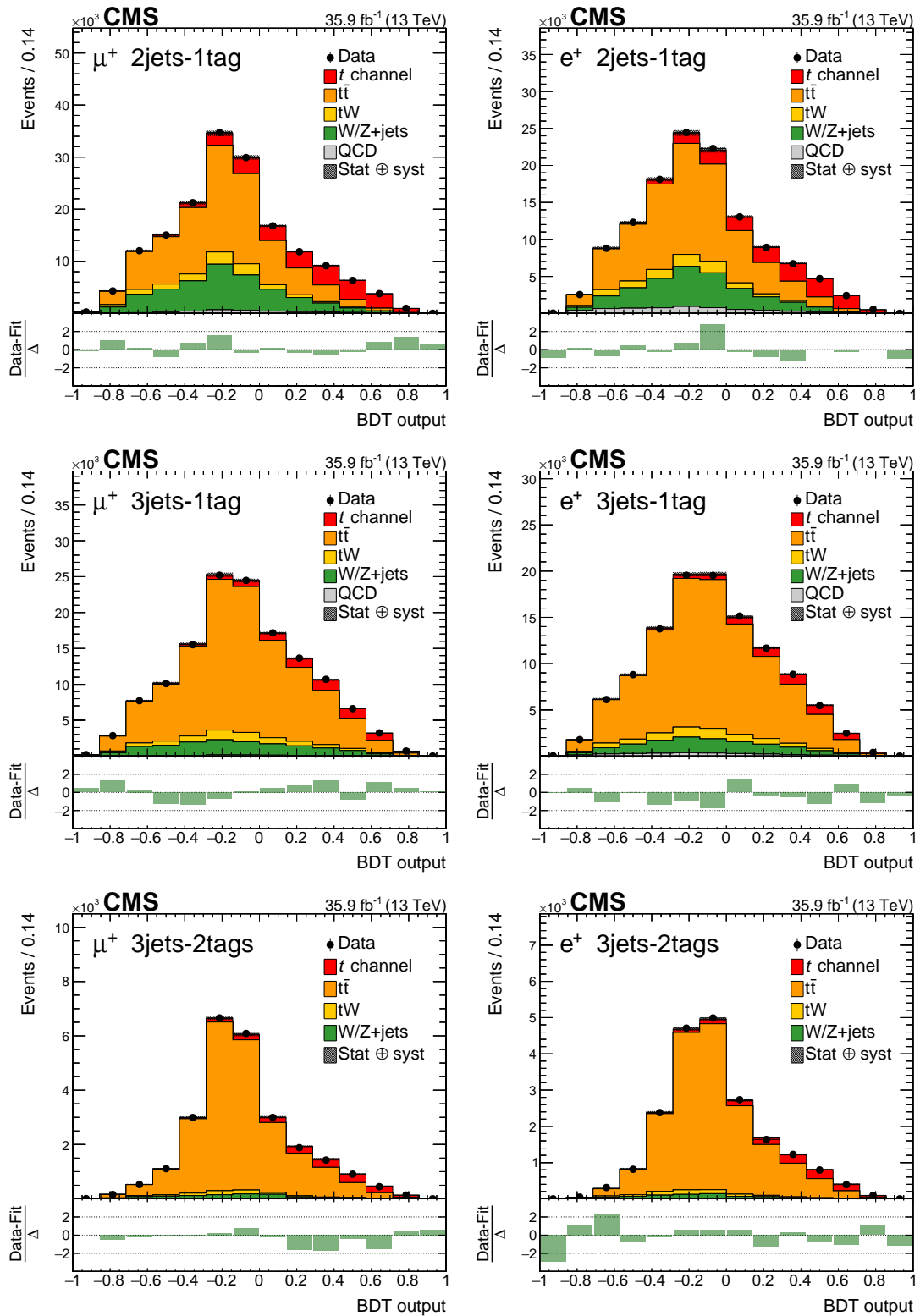
Figure 6: The BDT output distributions in the 2jets-1tag category (upper row), the 3jets-1tag category (middle row), and the 3jets-2tags category (lower row) for positively charged muons (left column) and electrons (right column). The different processes are scaled to the corresponding fit results. The shaded areas correspond to the uncertainties after performing the fit. In each figure, the pull is also shown.
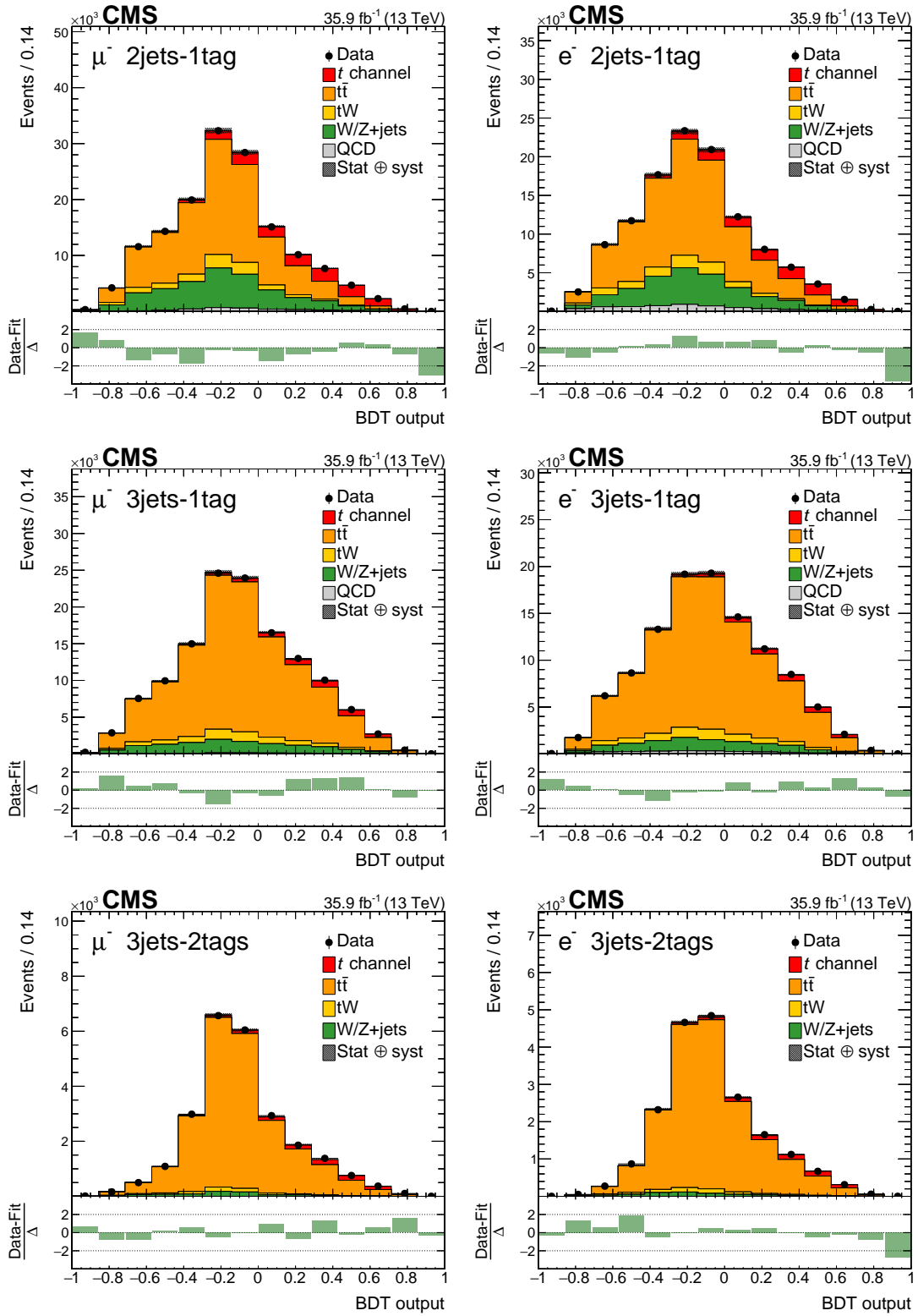
Figure 7: BDT output distributions in the 2jets-1tag category (upper row), the 3jets-1tag category (middle row), and the 3jets-2tags category (lower row) for negatively charged muons (left column) and electrons (right column). The different processes are scaled to the corresponding fit results. The shaded areas correspond to the uncertainties after performing the fit. In each figure, the pull is also shown.

Table 1: Input variables for the BDTs. The variables m_T^W and lepton $|\eta|$ are only used in the training of events with a muon, while p_T^{miss} is only considered as input for events with an electron.

Variable	Description
Light-quark jet $|\eta|$	Absolute value of the pseudorapidity of the light-quark jet
Top quark mass	Invariant mass of the top quark reconstructed from the lepton, the neutrino, and the b-tagged jet associated to the top quark decay
Dijet mass	Invariant mass of the light-quark jet and the b-tagged jet associated to the top quark decay
ΔR (lepton, b jet)	ΔR between the momentum vectors of the lepton and the b-tagged jet associated with the top quark decay
$\cos\theta^*$	Cosine of the angle between the lepton and the light-quark jet in the rest frame of the top quark
Jet p_T sum	Scalar sum of the transverse momenta of the light-quark jet and the b-tagged jet associated to the top quark decay
m_T^W	Transverse mass of the W boson
p_T^{miss}	Missing momentum in the transverse plane of the event
ΔR (light jet, b jet)	ΔR between the momentum vectors of the light-quark jet and the b-tagged jet associated to the top quark decay
Lepton $|\eta|$	Absolute value of the pseudorapidity of the selected lepton
W boson $|\eta|$	Absolute value of the pseudorapidity of the reconstructed W boson
Light-quark jet mass	Invariant mass of the light-quark jet

ples of simulated signal events that feature variations in the modeling parameters covering the systematic uncertainty sources under study.

- *Renormalization and factorization scales (shape):* The uncertainties caused by variations in the renormalization and factorization scales (μ_R / μ_F) are considered by applying weights [52], corresponding to simultaneously doubled or halved renormalization and factorization scales with the nominal value set to 172.5 GeV, on the BDT output distributions.

- *Matching of matrix element and parton shower (shape):* The parameter $h_{damp} = 1.581^{+0.658}_{-0.585} m_t$ (with $m_t = 172.5$ GeV) [38], which controls the matching between the matrix-element level calculation and the parton shower (ME-PS matching) and regulates the high-p_T radiation in the simulation, is varied within its uncertainties.

- *Parton shower scale (shape):* The renormalization scales of the initial-state and final-state parton shower (PS) are varied by factors of two and one half with the nominal value set to 172.5 GeV.

- *Signal PDFs (shape):* The impact due to the choice of PDFs is studied by replacing the nominal signal templates with reweighted distributions derived from the eigenvector variations of NNPDF3.0 NLO [39]. The full

envelope of the eigenvector variations is used.

- *Integrated luminosity (rate):* The relative uncertainty in the integrated luminosity is determined to be $\pm 2.5\%$ [53]. This uncertainty is added to the total uncertainties of the measured cross sections.

Profiled uncertainties

- *Jet energy scale (shape):* All reconstructed jet four-momenta are simultaneously varied in simulation according to the p_T- and η-dependent uncertainties in the jet energy scale (JES) [54]. In total, 26 different uncorrelated JES uncertainty sources are considered. These variations are also propagated to p_T^{miss}.

- *Jet energy resolution (shape):* To account for the difference in the jet energy resolution (JER) between data and simulation, a dedicated smearing is applied to the simulated jets [54], and the resolutions are varied within their uncertainties.

- *Unclustered energy (shape):* The contributions of unclustered PF candidates to p_T^{miss} are varied within their respective energy resolutions [55].

- b *tagging (shape):* The scale factors that are used to calculate the efficiency corrections of the CSVv2 b tagging algorithm are varied up and down within their uncertainties [47]. From these up and down varied scale factors, up and down shifted efficiency corrections are calculated and applied to the simulation.

- *Muon and electron efficiencies (shape):* The efficiencies of the lepton identification and isolation, of the trigger paths, and of the detector response are determined with a "tag-and-probe" method [56] from Drell–Yan events falling into the Z boson mass window. The efficiency correction factors are varied according to the p_T- and η-dependent uncertainties.

- *Pileup (shape):* The uncertainty in the average expected number of pileup interactions is propagated as a systematic uncertainty to this measurement by varying the total inelastic cross section by $\pm 4.6\%$ [57].

- *QCD background normalization (rate):* As described in Section 5, an uncertainty of $\pm 50\%$ is applied to the QCD background estimate to cover all effects from variations in the shape and rate of this process.

- *Limited size of samples of simulated events (shape):* The limited number of available simulated events is considered by performing the fit using the Barlow–Beeston method [58].

- t$\bar{\text{t}}$ *background modeling (shape) and normalization (rate):* Multiple systematic effects on the t$\bar{\text{t}}$ background prediction are studied: the influence of the parton shower scale and of the matching between the NLO calculation and the parton shower, the impact of variations in the initial- and final-state radiation—depending on the choice of α_S—and the effect of uncertainties in the modeling of the underlying event. Dedicated t$\bar{\text{t}}$ simulation samples are used to study each effect individually, where the corresponding parameters are varied within their uncertainties. To account for the uncertainty in the prediction of the inclusive t$\bar{\text{t}}$ cross section, a rate uncertainty of $\pm 6\%$ is applied [59].

- *Top quark p_T (shape):* In differential measurements of the top quark p_T in t$\bar{\text{t}}$ events, the predicted p_T spectrum is found to be harder than the observed spectrum [60, 61]. To account for this mismodeling, the results derived using the default simulation for t$\bar{\text{t}}$ are compared to the results using simulated t$\bar{\text{t}}$ events that are reweighted according to the observed difference between data and simulation. This results in one-sided

variations of the nominal template.

- tW *background normalization (rate):* To account for the uncertainty in the cross section of tW production and to cover a possible additional systematic uncertainty arising from the procedure which deals with the overlap with the $t\bar{t}$ process at NLO, a rate uncertainty of $\pm 11\%$, corresponding to the most precise measurement [62], is applied. One additional rate uncertainty is included in the fit to account for the impact from the choice of PDFs and their specific variation ($\pm 4\%$). To determine the influence of possible mismodeling of the tW process, the nominal sample is compared to samples generated with a parton shower scale shifted by ± 1 standard deviation.

- W/Z+*jets background normalization (rate):* To take the uncertainty in the cross sections of the W+jets and Z+jets contributions into account, as well as possible effects due to selecting heavy-flavored jets, individual rate uncertainties of $\pm 10\%$ are applied. By employing these uncertainties, a full evaluation of uncertainty sources for these processes is achieved, as well as a consistent treatment among the different background contributions.

- *Renormalization and factorization scales (shape):* For the background contributions from $t\bar{t}$, tW, and W/Z+jets production, the uncertainties caused by variations in the renormalization and factorization scales (μ_R/μ_F) are considered by reweighting [52] the BDT output distributions according to simultaneously doubled or halved renormalization and factorization scales. In the case of the $t\bar{t}$ and tW processes, the nominal value of the scales is set to $172.5\,\text{GeV}$, while dynamic scales, defined as $\sqrt{m_{W/Z}^2 + (p_T^{W/Z})^2}$, are used for W/Z+jets production. This uncertainty is estimated for each process separately.

- *Background PDFs (shape):* By reweighting distributions derived from the eigenvector variations of NNPDF3.0 NLO [39], the impact due to the choice of PDFs is studied for the $t\bar{t}$ and W/Z+jets background processes. The full envelope of the eigenvector variations is used. The variations in the background PDFs are treated as uncorrelated to the variations in the signal PDFs, because the dominant contributions to the signal PDFs stem from up and down quarks, whereas the background PDFs are dominated by gluons.

The by far largest contribution to the selected data set comes from the $t\bar{t}$ background. To understand this background as well as possible, the fit is performed simultaneously in different *n*jets-*m*tags categories. As a consequence, nuisance parameters for systematic uncertainties that can cause migrations of events between the different categories, like the $t\bar{t}$ modeling and the jet reconstruction uncertainties, get constrained by the fit. The impact of the individual systematic uncertainties on the measured cross sections and their ratio are listed in Table 2. For nonprofiled uncertainties, the change of the result due to the respective variation is listed. The impact of each profiled uncertainty is defined as the shift in the parameter of interest that is induced by repeating the fit with the corresponding nuisance parameter fixed at either one standard deviation above or below its post-fit value, with all other nuisance parameters treated as usual. Of the two resulting shifts always the larger one is taken as the impact. For Table 2 several nuisance parameters are grouped together by adding their impacts in quadrature.

The dominant uncertainties for the cross section measurements come from variations of the parton shower scale and from the matching between the matrix element and the parton shower employed in the signal modeling. The various uncertainties affect the two cross section measurements in a correlated way, which leads to a significant reduction of their impact when calculating the ratio. The strength of the cancellation depends on the correlation of the respec-

Table 2: Estimated relative impact of uncertainties in percent of the measured cross sections or cross section ratio.

	$\Delta R_{t\text{-ch}}/R_{t\text{-ch}}$	$\Delta\sigma/\sigma(\text{t})$	$\Delta\sigma/\sigma(\bar{\text{t}})$
Nonprofiled uncertainties			
$\mu_{\text{R}}/\mu_{\text{F}}$ scale t channel	1.5	6.1	5.0
ME-PS scale matching t channel	0.5	7.1	7.8
PS scale t channel	0.9	10.1	9.6
PDF t channel	3.0	3.1	5.8
Luminosity	—	2.5	2.5
Profiled uncertainties			
JES	0.9	1.5	1.8
JER	0.2	< 0.1	0.2
Unclustered energy	< 0.1	0.1	0.2
b tagging	0.1	1.1	1.2
Muon and electron efficiencies	0.2	0.8	0.6
Pileup	0.1	0.9	1.0
QCD bkg. normalization	< 0.1	0.1	0.1
MC sample size	2.5	2.2	3.2
$t\bar{t}$ bkg. model and normalization	0.2	0.6	0.6
Top quark p_{T}	< 0.1	< 0.1	< 0.1
tW bkg. normalization	0.1	0.5	0.6
W/Z+jets bkg. normalization	0.3	0.6	0.9
$\mu_{\text{R}}/\mu_{\text{F}}$ scale $t\bar{t}$, tW, W/Z+jets	0.1	0.2	0.3
PDF $t\bar{t}$, W/Z+jets	< 0.1	0.2	0.2

tive uncertainties and their impact on the two cross sections. For instance, the nonprofiled signal modeling uncertainties are highly correlated between the two cross sections and the only remaining uncertainty contribution in the ratio comes from the differences in the size of the impacts on the individual cross sections. The dominant uncertainty contributions in the ratio measurement are the uncertainty due to the choice of the PDF set for the t-channel signal model and the uncertainty due to the size of the simulation samples.

8 Results

The measured cross sections for the t-channel production of single top quarks and antiquarks are

$$\begin{aligned}
\sigma_{t\text{-ch,t}} &= 130 \pm 1\,(\text{stat}) \pm 4\,(\text{prof}) \pm 18\,(\text{sig-mod}) \pm 3\,(\text{lumi})\,\text{pb} \\
&= 130 \pm 1\,(\text{stat}) \pm 19\,(\text{syst})\,\text{pb} \\
&= 130 \pm 19\,\text{pb}, \\
\sigma_{t\text{-ch,}\bar{t}} &= 77 \pm 1\,(\text{stat}) \pm 2\,(\text{prof}) \pm 11\,(\text{sig-mod}) \pm 2\,(\text{lumi})\,\text{pb} \\
&= 77 \pm 1\,(\text{stat}) \pm 12\,(\text{syst})\,\text{pb} \\
&= 77 \pm 12\,\text{pb}.
\end{aligned}$$

Here, the uncertainty sources that are profiled in the fit, are labeled as "prof", the uncertainties on the signal modeling are labeled as "sig-mod", and the uncertainty due to the integrated luminosity measurement is labeled as "lumi". The total systematic uncertainty is obtained by adding the three uncertainty contributions in quadrature. Adding the $\sigma_{t\text{-ch,t}}$ and $\sigma_{t\text{-ch,}\bar{t}}$ results,

the total cross section is found to be

$$\sigma_{t\text{-ch},t+\bar{t}} = 207 \pm 2\,(\text{stat}) \pm 6\,(\text{prof}) \pm 29\,(\text{sig-mod}) \pm 5\,(\text{lumi})\,\text{pb}$$
$$= 207 \pm 2\,(\text{stat}) \pm 31\,(\text{syst})\,\text{pb}$$
$$= 207 \pm 31\,\text{pb},$$

where the statistical uncertainties are treated as uncorrelated and the systematic uncertainties as correlated between the $\sigma_{t\text{-ch},t}$ and $\sigma_{t\text{-ch},\bar{t}}$ measurements. The total cross section is used to calculate the absolute value of the CKM matrix element V_{tb}. Neglecting $|V_{td}|$ and $|V_{ts}|$ as they are significantly smaller than $|V_{tb}|$, and assuming that the top quark exclusively decays to a b quark and a W boson, leads to

$$|f_{LV}V_{tb}| = \sqrt{\frac{\sigma_{t\text{-ch},t+\bar{t}}}{\sigma_{t\text{-ch},t+\bar{t}}^{\text{theo}}}},$$

with the predicted SM value $\sigma_{t\text{-ch},t+\bar{t}}^{\text{theo}} = 217.0^{+6.6}_{-4.6}\,(\text{scale}) \pm 6.2\,(\text{PDF}+\alpha_S)\,\text{pb}$ [10, 11, 16] assuming $|V_{tb}| = 1$. The anomalous form factor f_{LV} takes the possible presence of an anomalous W t b coupling into account, with $f_{LV} = 1$ for the case in which the Wtb interaction is a left-handed weak SM coupling and $f_{LV} \neq 1$ for physics beyond the SM [63]. The measured cross section translates to

$$|f_{LV}V_{tb}| = 0.98 \pm 0.07\,(\text{exp}) \pm 0.02\,(\text{theo}).$$

The first uncertainty considers all uncertainties of the cross section measurement, while the second uncertainty is derived from the uncertainty of the theoretical SM prediction. Assuming the unitarity of the CKM matrix, a lower limit of 0.82 is determined in the Feldman–Cousins unified approach [64] for $|V_{tb}|$ at 95% confidence level.

The ratio of the cross sections for the production of single top quarks and antiquarks in the t channel is measured as

$$R_{t\text{-ch}} = 1.68 \pm 0.02\,(\text{stat}) \pm 0.02\,(\text{prof}) \pm 0.05\,(\text{sig-mod})$$
$$= 1.68 \pm 0.02\,(\text{stat}) \pm 0.05\,(\text{syst})$$
$$= 1.68 \pm 0.06.$$

The measured ratio is compared to the predictions using different PDF sets as shown in Fig. 8. Good agreement between the measurement and most predictions is found.

9 Summary

Events with one muon or electron and multiple jets in the final state are used to measure the cross sections for the t-channel production of single top quarks and antiquarks, and their ratio. The measured cross sections are $130 \pm 1\,(\text{stat}) \pm 19\,(\text{syst})\,\text{pb}$ for the production of single top quarks, $77 \pm 1\,(\text{stat}) \pm 12\,(\text{syst})\,\text{pb}$ for the production of single top antiquarks, and $207 \pm 2\,(\text{stat}) \pm 31\,(\text{syst})\,\text{pb}$ for the total production. The latter result is used to calculate the absolute value of the Cabibbo–Kobayashi–Maskawa matrix element $|f_{LV}V_{tb}| = 0.98 \pm 0.07\,(\text{exp}) \pm 0.02\,(\text{theo})$, including an anomalous form factor f_{LV}. The measured ratio of the cross sections of the two processes $R_{t\text{-ch}} = 1.68 \pm 0.02\,(\text{stat}) \pm 0.05\,(\text{syst})$ is compared to recent predictions using different parton distribution functions (PDFs) to describe the inner structure of the proton. Good agreement with most PDF sets is found within the uncertainties of the measurement.

The statistical uncertainty plays only a minor role for the achieved precision of the measurements, which are limited by the systematic uncertainties in the modeling of the signal process.
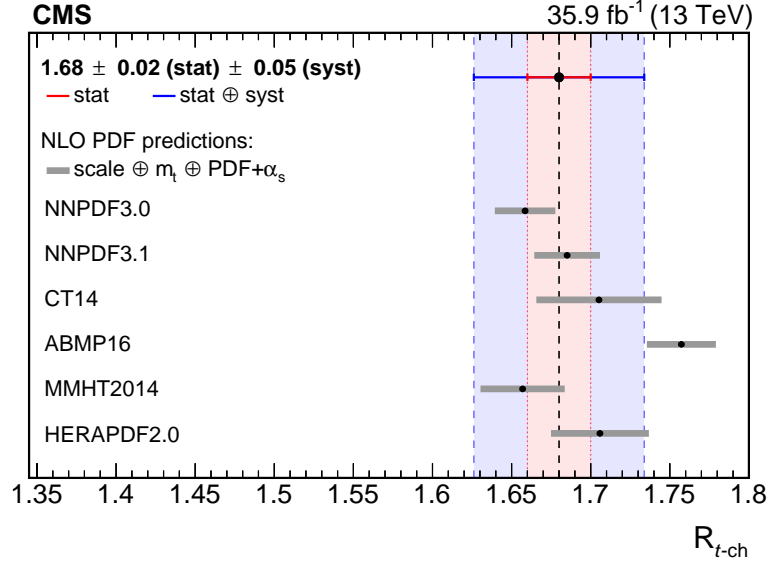
Figure 8: Comparison of the measured $R_{t\text{-ch}}$ (central dashed line) with the NLO predictions from different PDF sets, provided by LHAPDF 6.2.1 [65]: NNPDF3.0 [39], NNPDF3.1 [66], CT14 [67], ABMP16 [68, 69], MMHT2014 [70], HERAPDF2.0 [71]. The HATHOR 5FS calculation is used with the nominal values for the top quark pole mass and α_S set to the best values of each PDF set. The uncertainty bars for the different PDF sets include the uncertainty due to the factorization and renormalization scales, the uncertainty in the top quark pole mass, and the combined internal PDF+α_S uncertainty. For the measurement, the statistical and total uncertainties are indicated individually by the inner and outer uncertainty bars.

Deeper understanding of these effects and improved procedures to estimate the uncertainty are therefore crucial to further decrease the systematic uncertainty. Because of the cancellation of systematic effects when measuring the ratio of cross sections $R_{t\text{-ch}}$, its precision, reported in this letter, is significantly improved with respect to the results of previous measurements. The value of $R_{t\text{-ch}}$ can be used to test the predictions from different PDF sets for their compatibility with the data.

Acknowledgments

References

[1] U. Husemann, "Top-quark physics: Status and prospects", *Prog. Part. Nucl. Phys.* **95** (2017) 48, `doi:10.1016/j.ppnp.2017.03.002`.

[2] ATLAS Collaboration, "Measurement of the *t*-channel single top-quark production cross section in *pp* collisions at $\sqrt{s} = 7$ TeV with the ATLAS detector", *Phys. Lett. B* **717** (2012) 330, `doi:10.1016/j.physletb.2012.09.031`, `arXiv:1205.3130`.

[3] ATLAS Collaboration, "Comprehensive measurements of *t*-channel single top-quark production cross sections at $\sqrt{s} = 7$ TeV with the ATLAS detector", *Phys. Rev. D* **90** (2014) 112006, `doi:10.1103/PhysRevD.90.112006`, `arXiv:1406.7844`.

[4] ATLAS Collaboration, "Fiducial, total and differential cross-section measurements of *t*-channel single top-quark production in *pp* collisions at 8 TeV using data collected by the ATLAS detector", *Eur. Phys. J. C* **77** (2017) 531, `doi:10.1140/epjc/s10052-017-5061-9`, `arXiv:1702.02859`.

[5] ATLAS Collaboration, "Measurement of the inclusive cross-sections of single top-quark and top-antiquark *t*-channel production in *pp* collisions at $\sqrt{s} = 13$ TeV with the ATLAS detector", *JHEP* **04** (2017) 086, `doi:10.1007/JHEP04(2017)086`, `arXiv:1609.03920`.

[6] CMS Collaboration, "Measurement of the t-channel single top quark production cross section in pp collisions at $\sqrt{s} = 7$ TeV", *Phys. Rev. Lett.* **107** (2011) 091802, `doi:10.1103/PhysRevLett.107.091802`, `arXiv:1106.3052`.

[7] CMS Collaboration, "Measurement of the single-top-quark t-channel cross section in pp collisions at $\sqrt{s} = 7$ TeV", *JHEP* **12** (2012) 035, `doi:10.1007/JHEP12(2012)035`, `arXiv:1209.4533`.

[8] CMS Collaboration, "Measurement of the t-channel single-top-quark production cross section and of the $|V_{tb}|$ CKM matrix element in pp collisions at $\sqrt{s} = 8$ TeV", *JHEP* **06** (2014) 090, `doi:10.1007/JHEP06(2014)090`, `arXiv:1403.7366`.

[9] CMS Collaboration, "Cross section measurement of t-channel single top quark production in pp collisions at $\sqrt{s} = 13$ TeV", *Phys. Lett. B* **772** (2017) 752, `doi:10.1016/j.physletb.2017.07.047`, `arXiv:1610.00678`.

[10] M. Aliev et al., "HATHOR: HAdronic Top and Heavy quarks crOss section calculatoR", *Comput. Phys. Commun.* **182** (2011) 1034, `doi:10.1016/j.cpc.2010.12.040`, `arXiv:1007.1327`.

[11] P. Kant et al., "HatHor for single top-quark production: Updated predictions and uncertainty estimates for single top-quark production in hadronic collisions", *Comput. Phys. Commun.* **191** (2015) 74, `doi:10.1016/j.cpc.2015.02.001`, `arXiv:1406.4403`.

[12] A. D. Martin, W. J. Stirling, R. S. Thorne, and G. Watt, "Parton distributions for the LHC", *Eur. Phys. J. C* **63** (2009) 189, `doi:10.1140/epjc/s10052-009-1072-5`, `arXiv:0901.0002`.

[13] A. D. Martin, W. J. Stirling, R. S. Thorne, and G. Watt, "Uncertainties on α_S in global PDF analyses and implications for predicted hadronic cross sections", *Eur. Phys. J. C* **64** (2009) 653, `doi:10.1140/epjc/s10052-009-1164-2`, `arXiv:0905.3531`.

[14] H.-L. Lai et al., "New parton distributions for collider physics", *Phys. Rev. D* **82** (2010) 074024, `doi:10.1103/PhysRevD.82.074024`, `arXiv:1007.2241`.

[15] R. D. Ball et al., "Parton distributions with LHC data", *Nucl. Phys. B* **867** (2013) 244, `doi:10.1016/j.nuclphysb.2012.10.003`, `arXiv:1207.1303`.

[16] M. Botje et al., "The PDF4LHC Working Group Interim Recommendations", (2011). `arXiv:1101.0538`.

[17] S. Alekhin et al., "The PDF4LHC Working Group Interim Report", (2011). `arXiv:1101.0536`.

[18] E. L. Berger, J. Gao, C. P. Yuan, and H. X. Zhu, "NNLO QCD Corrections to t-channel Single Top-Quark Production and Decay", *Phys. Rev. D* **94** (2016) 071501, `doi:10.1103/PhysRevD.94.071501`, `arXiv:1606.08463`.

[19] CMS Collaboration, "The CMS trigger system", *JINST* **12** (2017) P01020, `doi:10.1088/1748-0221/12/01/P01020`, `arXiv:1609.02366`.

[20] CMS Collaboration, "The CMS experiment at the CERN LHC", *JINST* **3** (2008) S08004, `doi:10.1088/1748-0221/3/08/S08004`.

[21] J. Alwall et al., "The automated computation of tree-level and next-to-leading order differential cross sections, and their matching to parton shower simulations", *JHEP* **07** (2014) 079, `doi:10.1007/JHEP07(2014)079`, `arXiv:1405.0301`.

[22] S. Alioli, P. Nason, C. Oleari, and E. Re, "NLO single-top production matched with shower in POWHEG: s- and t-channel contributions", *JHEP* **09** (2009) 111, `doi:10.1088/1126-6708/2009/09/111`, `arXiv:0907.4076`.

[23] P. Nason, "A new method for combining NLO QCD with shower Monte Carlo algorithms", *JHEP* **11** (2004) 040, `doi:10.1088/1126-6708/2004/11/040`, `arXiv:hep-ph/0409146`.

[24] S. Frixione, P. Nason, and C. Oleari, "Matching NLO QCD computations with parton shower simulations: the POWHEG method", *JHEP* **11** (2007) 070, `doi:10.1088/1126-6708/2007/11/070`, `arXiv:0709.2092`.

[25] S. Alioli, P. Nason, C. Oleari, and E. Re, "A general framework for implementing NLO calculations in shower Monte Carlo programs: the POWHEG BOX", *JHEP* **06** (2010) 043, `doi:10.1007/JHEP06(2010)043`, `arXiv:1002.2581`.

[26] R. Frederix, E. Re, and P. Torrielli, "Single-top *t*-channel hadroproduction in the four-flavour scheme with POWHEG and aMC@NLO", *JHEP* **09** (2012) 130, `doi:10.1007/JHEP09(2012)130`, `arXiv:1207.5391`.

[27] S. Alioli, S.-O. Moch, and P. Uwer, "Hadronic top-quark pair-production with one jet and parton showering", *JHEP* **01** (2012) 137, `doi:10.1007/JHEP01(2012)137`, `arXiv:1110.5251`.

[28] M. Czakon and A. Mitov, "Top++: A program for the calculation of the top-pair cross-section at hadron colliders", *Comput. Phys. Commun.* **185** (2014) 2930, `doi:10.1016/j.cpc.2014.06.021`, `arXiv:1112.5675`.

[29] E. Re, "Single-top Wt-channel production matched with parton showers using the POWHEG method", *Eur. Phys. J. C* **71** (2011) 1547, `doi:10.1140/epjc/s10052-011-1547-z`, `arXiv:1009.2450`.

[30] N. Kidonakis, "Two-loop soft anomalous dimensions for single top quark associated production with a W- or H-", *Phys. Rev. D* **82** (2010) 054018, `doi:10.1103/PhysRevD.82.054018`, `arXiv:1005.4451`.

[31] N. Kidonakis, "Top quark production", in *Proceedings, Helmholtz International Summer School on Physics of Heavy Quarks and Hadrons (HQ 2013): JINR, Dubna, Russia, July 15-28, 2013*, p. 139. 2014. `arXiv:1311.0283`. `doi:10.3204/DESY-PROC-2013-03/Kidonakis`.

[32] R. Frederix and S. Frixione, "Merging meets matching in MC@NLO", *JHEP* **12** (2012) 061, `doi:10.1007/JHEP12(2012)061`, `arXiv:1209.6215`.

[33] R. Gavin, Y. Li, F. Petriello, and S. Quackenbush, "FEWZ 2.0: A code for hadronic Z production at next-to-next-to-leading order", *Comput. Phys. Commun.* **182** (2011) 2388, `doi:10.1016/j.cpc.2011.06.008`, `arXiv:1011.3540`.

[34] R. Gavin, Y. Li, F. Petriello, and S. Quackenbush, "W physics at the LHC with FEWZ 2.1", *Comput. Phys. Commun.* **184** (2013) 208, `doi:10.1016/j.cpc.2012.09.005`, `arXiv:1201.5896`.

[35] Y. Li and F. Petriello, "Combining QCD and electroweak corrections to dilepton production in FEWZ", *Phys. Rev. D* **86** (2012) 094034, `doi:10.1103/PhysRevD.86.094034`, `arXiv:1208.5967`.

[36] T. Sjöstrand et al., "An introduction to PYTHIA 8.2", *Comput. Phys. Commun.* **191** (2015) 159, `doi:10.1016/j.cpc.2015.01.024`, `arXiv:1410.3012`.

[37] CMS Collaboration, "Event generator tunes obtained from underlying event and multiparton scattering measurements", *Eur. Phys. J. C* **76** (2016) 155, `doi:10.1140/epjc/s10052-016-3988-x`, `arXiv:1512.00815`.

[38] CMS Collaboration, "Investigations of the impact of the parton shower tuning in Pythia 8 in the modelling of $t\bar{t}$ at $\sqrt{s} = 8$ and 13 TeV", CMS Physics Analysis Summary CMS-PAS-TOP-16-021, 2016.

[39] NNPDF Collaboration, "Parton distributions for the LHC Run II", *JHEP* **04** (2015) 040, `doi:10.1007/JHEP04(2015)040`, `arXiv:1410.8849`.

[40] GEANT4 Collaboration, "GEANT4—a simulation toolkit", *Nucl. Instrum. Meth. A* **506** (2003) 250, `doi:10.1016/S0168-9002(03)01368-8`.

[41] M. Cacciari, G. P. Salam, and G. Soyez, "The anti-k_T jet clustering algorithm", *JHEP* **04** (2008) 063, `doi:10.1088/1126-6708/2008/04/063`, `arXiv:0802.1189`.

[42] M. Cacciari, G. P. Salam, and G. Soyez, "FastJet user manual", *Eur. Phys. J. C* **72** (2012) 1896, `doi:10.1140/epjc/s10052-012-1896-2`, `arXiv:1111.6097`.

[43] CMS Collaboration, "Particle-flow reconstruction and global event description with the CMS detector", *JINST* **12** (2017) P10003, `doi:10.1088/1748-0221/12/10/P10003`, `arXiv:1706.04965`.

[44] CMS Collaboration, "Performance of the CMS muon detector and muon reconstruction with proton-proton collisions at $\sqrt{s} = 13$ TeV", *JINST* **13** (2018) P06015, `doi:10.1088/1748-0221/13/06/P06015`, `arXiv:1804.04528`.

[45] W. Adam, R. Frühwirth, A. Strandlie, and T. Todorov, "Reconstruction of electrons with the Gaussian-sum filter in the CMS tracker at the LHC", *J. Phys. G* **31** (2005) 9, `doi:10.1088/0954-3899/31/9/N01`, `arXiv:physics/0306087`.

[46] CMS Collaboration, "Jet energy scale and resolution in the CMS experiment in pp collisions at 8 TeV", *JINST* **12** (2017) P02014, `doi:10.1088/1748-0221/12/02/P02014`, `arXiv:1607.03663`.

[47] CMS Collaboration, "Identification of heavy-flavour jets with the CMS detector in pp collisions at 13 TeV", *JINST* **13** (2018) P05011, `doi:10.1088/1748-0221/13/05/P05011`, `arXiv:1712.07158`.

[48] CMS Collaboration, "Performance of missing energy reconstruction in 13 TeV pp collision data using the CMS detector", CMS Physics Analysis Summary CMS-PAS-JME-16-004, 2016.

[49] D0 Collaboration, "Observation of single top-quark production", *Phys. Rev. Lett.* **103** (2009) 092001, `doi:10.1103/PhysRevLett.103.092001`, `arXiv:0903.0850`.

[50] CDF Collaboration, "First observation of electroweak single top quark production", *Phys. Rev. Lett.* **103** (2009) 092002, `doi:10.1103/PhysRevLett.103.092002`, `arXiv:0903.0885`.

[51] J. Therhaag et al., "TMVA—toolkit for multivariate data analysis", in *Proceedings, Int'l Conf. on Computational Methods in Science and Engineering, 2009, ICCMSE2009*, volume 1504, p. 1013. 2012. `doi:10.1063/1.4771869`.

[52] A. Kalogeropoulos and J. Alwall, "The SysCalc code: A tool to derive theoretical systematic uncertainties", (2018). `arXiv:1801.08401`.

[53] CMS Collaboration, "CMS luminosity measurements for the 2016 data taking period", CMS Physics Analysis Summary CMS-PAS-LUM-17-001, 2017.

[54] CMS Collaboration, "Determination of jet energy calibration and transverse momentum resolution in CMS", *JINST* **6** (2011) P11002, `doi:10.1088/1748-0221/6/11/P11002`, `arXiv:1107.4277`.

[55] CMS Collaboration, "Performance of the CMS missing transverse momentum reconstruction in pp data at $\sqrt{s} = 8$ TeV", *JINST* **10** (2015) P02006, `doi:10.1088/1748-0221/10/02/P02006`, `arXiv:1411.0511`.

[56] CMS Collaboration, "Measurements of inclusive W and Z cross sections in pp collisions at $\sqrt{s} = 7$ TeV", *JHEP* **01** (2011) 080, `doi:10.1007/JHEP01(2011)080`, `arXiv:1012.2466`.

[57] CMS Collaboration, "Measurement of the inelastic proton-proton cross section at $\sqrt{s} = 13$ TeV", *JHEP* **07** (2018) 161, `doi:10.1007/JHEP07(2018)161`, `arXiv:1802.02613`.

[58] R. Barlow and C. Beeston, "Fitting using finite Monte Carlo samples", *Comp. Phys. Commun.* **77** (1993) 219, `doi:10.1016/0010-4655(93)90005-W`.

[59] M. Czakon, P. Fiedler, and A. Mitov, "Total top-quark pair-production cross section at hadron colliders through $O(\alpha_S^4)$", *Phys. Rev. Lett.* **110** (2013) 252004, `doi:10.1103/PhysRevLett.110.252004`, `arXiv:1303.6254`.

[60] CMS Collaboration, "Measurement of differential cross sections for top quark pair production using the lepton+jets final state in proton-proton collisions at 13 TeV", *Phys. Rev. D* **95** (2017) 092001, `doi:10.1103/PhysRevD.95.092001`, `arXiv:1610.04191`.

[61] CMS Collaboration, "Measurement of normalized differential t$\bar{\text{t}}$ cross sections in the dilepton channel from pp collisions at $\sqrt{s} = 13$ TeV", *JHEP* **04** (2018) 060, `doi:10.1007/JHEP04(2018)060`, `arXiv:1708.07638`.

[62] CMS Collaboration, "Measurement of the production cross section for single top quarks in association with W bosons in proton-proton collisions at $\sqrt{s} = 13$ TeV", *JHEP* **10** (2018) 117, `doi:10.1007/JHEP10(2018)117`, `arXiv:1805.07399`.

[63] J. A. Aguilar-Saavedra, "A Minimal set of top anomalous couplings", *Nucl. Phys. B* **812** (2009) 181, `doi:10.1016/j.nuclphysb.2008.12.012`, `arXiv:0811.3842`.

[64] G. J. Feldman and R. D. Cousins, "A Unified approach to the classical statistical analysis of small signals", *Phys. Rev. D* **57** (1998) 3873, `doi:10.1103/PhysRevD.57.3873`, `arXiv:physics/9711021`.

[65] A. Buckley et al., "LHAPDF6: parton density access in the LHC precision era", *Eur. Phys. J. C* **75** (2015) 132, `doi:10.1140/epjc/s10052-015-3318-8`, `arXiv:1412.7420`.

[66] NNPDF Collaboration, "Parton distributions from high-precision collider data", *Eur. Phys. J. C* **77** (2017) 663, `doi:10.1140/epjc/s10052-017-5199-5`, `arXiv:1706.00428`.

[67] S. Dulat et al., "New parton distribution functions from a global analysis of quantum chromodynamics", *Phys. Rev. D* **93** (2016) 033006, `doi:10.1103/PhysRevD.93.033006`, `arXiv:1506.07443`.

[68] S. Alekhin, J. Blümlein, S.-O. Moch, and R. Placakyte, "Parton distribution functions, α_s, and heavy-quark masses for LHC Run II", *Phys. Rev. D* **96** (2017) 014011, `doi:10.1103/PhysRevD.96.014011`, `arXiv:1701.05838`.

[69] S. Alekhin, J. Blümlein, and S.-O. Moch, "NLO PDFs from the ABMP16 fit", *Eur. Phys. J. C* **78** (2018) 477, `doi:10.1140/epjc/s10052-018-5947-1`, `arXiv:1803.07537`.

[70] L. A. Harland-Lang, A. D. Martin, P. Motylinski, and R. S. Thorne, "Parton distributions in the LHC era: MMHT 2014 PDFs", *Eur. Phys. J. C* **75** (2015) 204, `doi:10.1140/epjc/s10052-015-3397-6`, `arXiv:1412.3989`.

[71] ZEUS and H1 Collaborations, "Combined measurement and QCD analysis of the inclusive $e^{\pm}p$ scattering cross sections at HERA", *JHEP* **01** (2010) 109, `doi:10.1007/JHEP01(2010)109`, `arXiv:0911.0884`.

A   The CMS Collaboration

Yerevan Physics Institute, Yerevan, Armenia
A.M. Sirunyan, A. Tumasyan

Institut für Hochenergiephysik, Wien, Austria
W. Adam, F. Ambrogi, E. Asilar, T. Bergauer, J. Brandstetter, M. Dragicevic, J. Erö, A. Escalante Del Valle, M. Flechl, R. Frühwirth[1], V.M. Ghete, J. Hrubec, M. Jeitler[1], N. Krammer, I. Krätschmer, D. Liko, T. Madlener, I. Mikulec, N. Rad, H. Rohringer, J. Schieck[1], R. Schöfbeck, M. Spanring, D. Spitzbart, A. Taurok, W. Waltenberger, J. Wittmann, C.-E. Wulz[1], M. Zarucki

Institute for Nuclear Problems, Minsk, Belarus
V. Chekhovsky, V. Mossolov, J. Suarez Gonzalez

Universiteit Antwerpen, Antwerpen, Belgium
E.A. De Wolf, D. Di Croce, X. Janssen, J. Lauwers, M. Pieters, H. Van Haevermaet, P. Van Mechelen, N. Van Remortel

Vrije Universiteit Brussel, Brussel, Belgium
S. Abu Zeid, F. Blekman, J. D'Hondt, J. De Clercq, K. Deroover, G. Flouris, D. Lontkovskyi, S. Lowette, I. Marchesini, S. Moortgat, L. Moreels, Q. Python, K. Skovpen, S. Tavernier, W. Van Doninck, P. Van Mulders, I. Van Parijs

Université Libre de Bruxelles, Bruxelles, Belgium
D. Beghin, B. Bilin, H. Brun, B. Clerbaux, G. De Lentdecker, H. Delannoy, B. Dorney, G. Fasanella, L. Favart, R. Goldouzian, A. Grebenyuk, A.K. Kalsi, T. Lenzi, J. Luetic, N. Postiau, E. Starling, L. Thomas, C. Vander Velde, P. Vanlaer, D. Vannerom, Q. Wang

Ghent University, Ghent, Belgium
T. Cornelis, D. Dobur, A. Fagot, M. Gul, I. Khvastunov[2], D. Poyraz, C. Roskas, D. Trocino, M. Tytgat, W. Verbeke, B. Vermassen, M. Vit, N. Zaganidis

Université Catholique de Louvain, Louvain-la-Neuve, Belgium
H. Bakhshiansohi, O. Bondu, S. Brochet, G. Bruno, C. Caputo, P. David, C. Delaere, M. Delcourt, A. Giammanco, G. Krintiras, V. Lemaitre, A. Magitteri, K. Piotrzkowski, A. Saggio, M. Vidal Marono, S. Wertz, J. Zobec

Centro Brasileiro de Pesquisas Fisicas, Rio de Janeiro, Brazil
F.L. Alves, G.A. Alves, M. Correa Martins Junior, G. Correia Silva, C. Hensel, A. Moraes, M.E. Pol, P. Rebello Teles

Universidade do Estado do Rio de Janeiro, Rio de Janeiro, Brazil
E. Belchior Batista Das Chagas, W. Carvalho, J. Chinellato[3], E. Coelho, E.M. Da Costa, G.G. Da Silveira[4], D. De Jesus Damiao, C. De Oliveira Martins, S. Fonseca De Souza, H. Malbouisson, D. Matos Figueiredo, M. Melo De Almeida, C. Mora Herrera, L. Mundim, H. Nogima, W.L. Prado Da Silva, L.J. Sanchez Rosas, A. Santoro, A. Sznajder, M. Thiel, E.J. Tonelli Manganote[3], F. Torres Da Silva De Araujo, A. Vilela Pereira

Universidade Estadual Paulista ^{a}, Universidade Federal do ABC ^{b}, São Paulo, Brazil
S. Ahuja^a, C.A. Bernardes^a, L. Calligaris^a, T.R. Fernandez Perez Tomei^a, E.M. Gregores^b, P.G. Mercadante^b, S.F. Novaes^a, SandraS. Padula^a

Institute for Nuclear Research and Nuclear Energy, Bulgarian Academy of Sciences, Sofia,

Bulgaria
A. Aleksandrov, R. Hadjiiska, P. Iaydjiev, A. Marinov, M. Misheva, M. Rodozov, M. Shopova, G. Sultanov

University of Sofia, Sofia, Bulgaria
A. Dimitrov, L. Litov, B. Pavlov, P. Petkov

Beihang University, Beijing, China
W. Fang[5], X. Gao[5], L. Yuan

Institute of High Energy Physics, Beijing, China
M. Ahmad, J.G. Bian, G.M. Chen, H.S. Chen, M. Chen, Y. Chen, C.H. Jiang, D. Leggat, H. Liao, Z. Liu, F. Romeo, S.M. Shaheen[6], A. Spiezia, J. Tao, Z. Wang, E. Yazgan, H. Zhang, S. Zhang[6], J. Zhao

State Key Laboratory of Nuclear Physics and Technology, Peking University, Beijing, China
Y. Ban, G. Chen, A. Levin, J. Li, L. Li, Q. Li, Y. Mao, S.J. Qian, D. Wang

Tsinghua University, Beijing, China
Y. Wang

Universidad de Los Andes, Bogota, Colombia
C. Avila, A. Cabrera, C.A. Carrillo Montoya, L.F. Chaparro Sierra, C. Florez, C.F. González Hernández, M.A. Segura Delgado

University of Split, Faculty of Electrical Engineering, Mechanical Engineering and Naval Architecture, Split, Croatia
B. Courbon, N. Godinovic, D. Lelas, I. Puljak, T. Sculac

University of Split, Faculty of Science, Split, Croatia
Z. Antunovic, M. Kovac

Institute Rudjer Boskovic, Zagreb, Croatia
V. Brigljevic, D. Ferencek, K. Kadija, B. Mesic, A. Starodumov[7], T. Susa

University of Cyprus, Nicosia, Cyprus
M.W. Ather, A. Attikis, M. Kolosova, G. Mavromanolakis, J. Mousa, C. Nicolaou, F. Ptochos, P.A. Razis, H. Rykaczewski

Charles University, Prague, Czech Republic
M. Finger[8], M. Finger Jr.[8]

Escuela Politecnica Nacional, Quito, Ecuador
E. Ayala

Universidad San Francisco de Quito, Quito, Ecuador
E. Carrera Jarrin

Academy of Scientific Research and Technology of the Arab Republic of Egypt, Egyptian Network of High Energy Physics, Cairo, Egypt
H. Abdalla[9], A.A. Abdelalim[10,11], A. Mohamed[11]

National Institute of Chemical Physics and Biophysics, Tallinn, Estonia
S. Bhowmik, A. Carvalho Antunes De Oliveira, R.K. Dewanjee, K. Ehataht, M. Kadastik, M. Raidal, C. Veelken

Department of Physics, University of Helsinki, Helsinki, Finland
P. Eerola, H. Kirschenmann, J. Pekkanen, M. Voutilainen

Helsinki Institute of Physics, Helsinki, Finland
J. Havukainen, J.K. Heikkilä, T. Järvinen, V. Karimäki, R. Kinnunen, T. Lampén, K. Lassila-Perini, S. Laurila, S. Lehti, T. Lindén, P. Luukka, T. Mäenpää, H. Siikonen, E. Tuominen, J. Tuominiemi

Lappeenranta University of Technology, Lappeenranta, Finland
T. Tuuva

IRFU, CEA, Université Paris-Saclay, Gif-sur-Yvette, France
M. Besancon, F. Couderc, M. Dejardin, D. Denegri, J.L. Faure, F. Ferri, S. Ganjour, A. Givernaud, P. Gras, G. Hamel de Monchenault, P. Jarry, C. Leloup, E. Locci, J. Malcles, G. Negro, J. Rander, A. Rosowsky, M.Ö. Sahin, M. Titov

Laboratoire Leprince-Ringuet, Ecole polytechnique, CNRS/IN2P3, Université Paris-Saclay, Palaiseau, France
A. Abdulsalam[12], C. Amendola, I. Antropov, F. Beaudette, P. Busson, C. Charlot, R. Granier de Cassagnac, I. Kucher, A. Lobanov, J. Martin Blanco, C. Martin Perez, M. Nguyen, C. Ochando, G. Ortona, P. Paganini, P. Pigard, J. Rembser, R. Salerno, J.B. Sauvan, Y. Sirois, A.G. Stahl Leiton, A. Zabi, A. Zghiche

Université de Strasbourg, CNRS, IPHC UMR 7178, Strasbourg, France
J.-L. Agram[13], J. Andrea, D. Bloch, J.-M. Brom, E.C. Chabert, V. Cherepanov, C. Collard, E. Conte[13], J.-C. Fontaine[13], D. Gelé, U. Goerlach, M. Jansová, A.-C. Le Bihan, N. Tonon, P. Van Hove

Centre de Calcul de l'Institut National de Physique Nucleaire et de Physique des Particules, CNRS/IN2P3, Villeurbanne, France
S. Gadrat

Université de Lyon, Université Claude Bernard Lyon 1, CNRS-IN2P3, Institut de Physique Nucléaire de Lyon, Villeurbanne, France
S. Beauceron, C. Bernet, G. Boudoul, N. Chanon, R. Chierici, D. Contardo, P. Depasse, H. El Mamouni, J. Fay, L. Finco, S. Gascon, M. Gouzevitch, G. Grenier, B. Ille, F. Lagarde, I.B. Laktineh, H. Lattaud, M. Lethuillier, L. Mirabito, S. Perries, A. Popov[14], V. Sordini, G. Touquet, M. Vander Donckt, S. Viret

Georgian Technical University, Tbilisi, Georgia
T. Toriashvili[15]

Tbilisi State University, Tbilisi, Georgia
Z. Tsamalaidze[8]

RWTH Aachen University, I. Physikalisches Institut, Aachen, Germany
C. Autermann, L. Feld, M.K. Kiesel, K. Klein, M. Lipinski, M. Preuten, M.P. Rauch, C. Schomakers, J. Schulz, M. Teroerde, B. Wittmer

RWTH Aachen University, III. Physikalisches Institut A, Aachen, Germany
A. Albert, D. Duchardt, M. Erdmann, S. Erdweg, T. Esch, R. Fischer, S. Ghosh, A. Güth, T. Hebbeker, C. Heidemann, K. Hoepfner, H. Keller, L. Mastrolorenzo, M. Merschmeyer, A. Meyer, P. Millet, S. Mukherjee, T. Pook, M. Radziej, H. Reithler, M. Rieger, A. Schmidt, D. Teyssier, S. Thüer

RWTH Aachen University, III. Physikalisches Institut B, Aachen, Germany
G. Flügge, O. Hlushchenko, T. Kress, T. Müller, A. Nehrkorn, A. Nowack, C. Pistone, O. Pooth, D. Roy, H. Sert, A. Stahl[16]

Deutsches Elektronen-Synchrotron, Hamburg, Germany
M. Aldaya Martin, T. Arndt, C. Asawatangtrakuldee, I. Babounikau, K. Beernaert, O. Behnke, U. Behrens, A. Bermúdez Martínez, D. Bertsche, A.A. Bin Anuar, K. Borras[17], V. Botta, A. Campbell, P. Connor, C. Contreras-Campana, V. Danilov, A. De Wit, M.M. Defranchis, C. Diez Pardos, D. Domínguez Damiani, G. Eckerlin, T. Eichhorn, A. Elwood, E. Eren, E. Gallo[18], A. Geiser, J.M. Grados Luyando, A. Grohsjean, M. Guthoff, M. Haranko, A. Harb, J. Hauk, H. Jung, M. Kasemann, J. Keaveney, C. Kleinwort, J. Knolle, D. Krücker, W. Lange, A. Lelek, T. Lenz, J. Leonard, K. Lipka, W. Lohmann[19], R. Mankel, I.-A. Melzer-Pellmann, A.B. Meyer, M. Meyer, M. Missiroli, G. Mittag, J. Mnich, V. Myronenko, S.K. Pflitsch, D. Pitzl, A. Raspereza, M. Savitskyi, P. Saxena, P. Schütze, C. Schwanenberger, R. Shevchenko, A. Singh, H. Tholen, O. Turkot, A. Vagnerini, G.P. Van Onsem, R. Walsh, Y. Wen, K. Wichmann, C. Wissing, O. Zenaiev

University of Hamburg, Hamburg, Germany
R. Aggleton, S. Bein, L. Benato, A. Benecke, V. Blobel, T. Dreyer, A. Ebrahimi, E. Garutti, D. Gonzalez, P. Gunnellini, J. Haller, A. Hinzmann, A. Karavdina, G. Kasieczka, R. Klanner, R. Kogler, N. Kovalchuk, S. Kurz, V. Kutzner, J. Lange, D. Marconi, J. Multhaup, M. Niedziela, C.E.N. Niemeyer, D. Nowatschin, A. Perieanu, A. Reimers, O. Rieger, C. Scharf, P. Schleper, S. Schumann, J. Schwandt, J. Sonneveld, H. Stadie, G. Steinbrück, F.M. Stober, M. Stöver, A. Vanhoefer, B. Vormwald, I. Zoi

Karlsruher Institut fuer Technologie, Karlsruhe, Germany
M. Akbiyik, C. Barth, M. Baselga, S. Baur, E. Butz, R. Caspart, T. Chwalek, F. Colombo, W. De Boer, A. Dierlamm, K. El Morabit, N. Faltermann, B. Freund, M. Giffels, M.A. Harrendorf, F. Hartmann[16], S.M. Heindl, U. Husemann, I. Katkov[14], S. Kudella, S. Mitra, M.U. Mozer, D. Müller, Th. Müller, M. Musich, P. Ott, T. Pambor, M. Plagge, G. Quast, K. Rabbertz, M. Schröder, D. Seith, I. Shvetsov, H.J. Simonis, R. Ulrich, S. Wayand, M. Weber, T. Weiler, C. Wöhrmann, R. Wolf

Institute of Nuclear and Particle Physics (INPP), NCSR Demokritos, Aghia Paraskevi, Greece
G. Anagnostou, G. Daskalakis, T. Geralis, A. Kyriakis, D. Loukas, G. Paspalaki

National and Kapodistrian University of Athens, Athens, Greece
G. Karathanasis, P. Kontaxakis, A. Panagiotou, I. Papavergou, N. Saoulidou, E. Tziaferi, K. Vellidis

National Technical University of Athens, Athens, Greece
K. Kousouris, I. Papakrivopoulos, G. Tsipolitis

University of Ioánnina, Ioánnina, Greece
I. Evangelou, C. Foudas, P. Gianneios, P. Katsoulis, P. Kokkas, S. Mallios, N. Manthos, I. Papadopoulos, E. Paradas, J. Strologas, F.A. Triantis, D. Tsitsonis

MTA-ELTE Lendület CMS Particle and Nuclear Physics Group, Eötvös Loránd University, Budapest, Hungary
M. Bartók[20], M. Csanad, N. Filipovic, P. Major, M.I. Nagy, G. Pasztor, O. Surányi, G.I. Veres

Wigner Research Centre for Physics, Budapest, Hungary

G. Bencze, C. Hajdu, D. Horvath[21], Á. Hunyadi, F. Sikler, T.Á. Vámi, V. Veszpremi, G. Vesztergombi[†]

Institute of Nuclear Research ATOMKI, Debrecen, Hungary
N. Beni, S. Czellar, J. Karancsi[20], A. Makovec, J. Molnar, Z. Szillasi

Institute of Physics, University of Debrecen, Debrecen, Hungary
P. Raics, Z.L. Trocsanyi, B. Ujvari

Indian Institute of Science (IISc), Bangalore, India
S. Choudhury, J.R. Komaragiri, P.C. Tiwari

National Institute of Science Education and Research, HBNI, Bhubaneswar, India
S. Bahinipati[23], C. Kar, P. Mal, K. Mandal, A. Nayak[24], D.K. Sahoo[23], S.K. Swain

Panjab University, Chandigarh, India
S. Bansal, S.B. Beri, V. Bhatnagar, S. Chauhan, R. Chawla, N. Dhingra, R. Gupta, A. Kaur, M. Kaur, S. Kaur, P. Kumari, M. Lohan, A. Mehta, K. Sandeep, S. Sharma, J.B. Singh, A.K. Virdi, G. Walia

University of Delhi, Delhi, India
A. Bhardwaj, B.C. Choudhary, R.B. Garg, M. Gola, S. Keshri, Ashok Kumar, S. Malhotra, M. Naimuddin, P. Priyanka, K. Ranjan, Aashaq Shah, R. Sharma

Saha Institute of Nuclear Physics, HBNI, Kolkata, India
R. Bhardwaj[25], M. Bharti[25], R. Bhattacharya, S. Bhattacharya, U. Bhawandeep[25], D. Bhowmik, S. Dey, S. Dutt[25], S. Dutta, S. Ghosh, K. Mondal, S. Nandan, A. Purohit, P.K. Rout, A. Roy, S. Roy Chowdhury, G. Saha, S. Sarkar, M. Sharan, B. Singh[25], S. Thakur[25]

Indian Institute of Technology Madras, Madras, India
P.K. Behera

Bhabha Atomic Research Centre, Mumbai, India
R. Chudasama, D. Dutta, V. Jha, V. Kumar, P.K. Netrakanti, L.M. Pant, P. Shukla

Tata Institute of Fundamental Research-A, Mumbai, India
T. Aziz, M.A. Bhat, S. Dugad, G.B. Mohanty, N. Sur, B. Sutar, RavindraKumar Verma

Tata Institute of Fundamental Research-B, Mumbai, India
S. Banerjee, S. Bhattacharya, S. Chatterjee, P. Das, M. Guchait, Sa. Jain, S. Karmakar, S. Kumar, M. Maity[26], G. Majumder, K. Mazumdar, N. Sahoo, T. Sarkar[26]

Indian Institute of Science Education and Research (IISER), Pune, India
S. Chauhan, S. Dube, V. Hegde, A. Kapoor, K. Kothekar, S. Pandey, A. Rane, A. Rastogi, S. Sharma

Institute for Research in Fundamental Sciences (IPM), Tehran, Iran
S. Chenarani[27], E. Eskandari Tadavani, S.M. Etesami[27], M. Khakzad, M. Mohammadi Najafabadi, M. Naseri, F. Rezaei Hosseinabadi, B. Safarzadeh[28], M. Zeinali

University College Dublin, Dublin, Ireland
M. Felcini, M. Grunewald

INFN Sezione di Bari [a], **Università di Bari** [b], **Politecnico di Bari** [c], **Bari, Italy**
M. Abbrescia[a,b], C. Calabria[a,b], A. Colaleo[a], D. Creanza[a,c], L. Cristella[a,b], N. De Filippis[a,c], M. De Palma[a,b], A. Di Florio[a,b], F. Errico[a,b], L. Fiore[a], A. Gelmi[a,b], G. Iaselli[a,c], M. Ince[a,b], S. Lezki[a,b], G. Maggi[a,c], M. Maggi[a], G. Miniello[a,b], S. My[a,b], S. Nuzzo[a,b], A. Pompili[a,b],

G. Pugliese[a,c], R. Radogna[a], A. Ranieri[a], G. Selvaggi[a,b], A. Sharma[a], L. Silvestris[a], R. Venditti[a], P. Verwilligen[a], G. Zito[a]

INFN Sezione di Bologna [a], Università di Bologna [b], Bologna, Italy
G. Abbiendi[a], C. Battilana[a,b], D. Bonacorsi[a,b], L. Borgonovi[a,b], S. Braibant-Giacomelli[a,b], R. Campanini[a,b], P. Capiluppi[a,b], A. Castro[a,b], F.R. Cavallo[a], S.S. Chhibra[a,b], C. Ciocca[a], G. Codispoti[a,b], M. Cuffiani[a,b], G.M. Dallavalle[a], F. Fabbri[a], A. Fanfani[a,b], E. Fontanesi, P. Giacomelli[a], C. Grandi[a], L. Guiducci[a,b], F. Iemmi[a,b], S. Lo Meo[a], S. Marcellini[a], G. Masetti[a], A. Montanari[a], F.L. Navarria[a,b], A. Perrotta[a], F. Primavera[a,b,16], T. Rovelli[a,b], G.P. Siroli[a,b], N. Tosi[a]

INFN Sezione di Catania [a], Università di Catania [b], Catania, Italy
S. Albergo[a,b], A. Di Mattia[a], R. Potenza[a,b], A. Tricomi[a,b], C. Tuve[a,b]

INFN Sezione di Firenze [a], Università di Firenze [b], Firenze, Italy
G. Barbagli[a], K. Chatterjee[a,b], V. Ciulli[a,b], C. Civinini[a], R. D'Alessandro[a,b], E. Focardi[a,b], G. Latino, P. Lenzi[a,b], M. Meschini[a], S. Paoletti[a], L. Russo[a,29], G. Sguazzoni[a], D. Strom[a], L. Viliani[a]

INFN Laboratori Nazionali di Frascati, Frascati, Italy
L. Benussi, S. Bianco, F. Fabbri, D. Piccolo

INFN Sezione di Genova [a], Università di Genova [b], Genova, Italy
F. Ferro[a], R. Mulargia[a,b], F. Ravera[a,b], E. Robutti[a], S. Tosi[a,b]

INFN Sezione di Milano-Bicocca [a], Università di Milano-Bicocca [b], Milano, Italy
A. Benaglia[a], A. Beschi[b], F. Brivio[a,b], V. Ciriolo[a,b,16], S. Di Guida[a,d,16], M.E. Dinardo[a,b], S. Fiorendi[a,b], S. Gennai[a], A. Ghezzi[a,b], P. Govoni[a,b], M. Malberti[a,b], S. Malvezzi[a], A. Massironi[a,b], D. Menasce[a], F. Monti, L. Moroni[a], M. Paganoni[a,b], D. Pedrini[a], S. Ragazzi[a,b], T. Tabarelli de Fatis[a,b], D. Zuolo[a,b]

INFN Sezione di Napoli [a], Università di Napoli 'Federico II' [b], Napoli, Italy, Università della Basilicata [c], Potenza, Italy, Università G. Marconi [d], Roma, Italy
S. Buontempo[a], N. Cavallo[a,c], A. De Iorio[a,b], A. Di Crescenzo[a,b], F. Fabozzi[a,c], F. Fienga[a], G. Galati[a], A.O.M. Iorio[a,b], W.A. Khan[a], L. Lista[a], S. Meola[a,d,16], P. Paolucci[a,16], C. Sciacca[a,b], E. Voevodina[a,b]

INFN Sezione di Padova [a], Università di Padova [b], Padova, Italy, Università di Trento [c], Trento, Italy
P. Azzi[a], N. Bacchetta[a], D. Bisello[a,b], A. Boletti[a,b], A. Bragagnolo, R. Carlin[a,b], P. Checchia[a], M. Dall'Osso[a,b], P. De Castro Manzano[a], T. Dorigo[a], U. Dosselli[a], F. Gasparini[a,b], U. Gasparini[a,b], A. Gozzelino[a], S.Y. Hoh, S. Lacaprara[a], P. Lujan, M. Margoni[a,b], A.T. Meneguzzo[a,b], J. Pazzini[a,b], P. Ronchese[a,b], R. Rossin[a,b], F. Simonetto[a,b], A. Tiko, E. Torassa[a], M. Tosi[a,b], M. Zanetti[a,b], P. Zotto[a,b], G. Zumerle[a,b]

INFN Sezione di Pavia [a], Università di Pavia [b], Pavia, Italy
A. Braghieri[a], A. Magnani[a], P. Montagna[a,b], S.P. Ratti[a,b], V. Re[a], M. Ressegotti[a,b], C. Riccardi[a,b], P. Salvini[a], I. Vai[a,b], P. Vitulo[a,b]

INFN Sezione di Perugia [a], Università di Perugia [b], Perugia, Italy
M. Biasini[a,b], G.M. Bilei[a], C. Cecchi[a,b], D. Ciangottini[a,b], L. Fanò[a,b], P. Lariccia[a,b], R. Leonardi[a,b], E. Manoni[a], G. Mantovani[a,b], V. Mariani[a,b], M. Menichelli[a], A. Rossi[a,b], A. Santocchia[a,b], D. Spiga[a]

INFN Sezione di Pisa ^{a}, Università di Pisa ^{b}, Scuola Normale Superiore di Pisa ^{c}, Pisa, Italy
K. Androsov^a, P. Azzurri^a, G. Bagliesi^a, L. Bianchini^a, T. Boccali^a, L. Borrello, R. Castaldi^a, M.A. Ciocci^{a,b}, R. Dell'Orso^a, G. Fedi^a, F. Fiori^{a,c}, L. Giannini^{a,c}, A. Giassi^a, M.T. Grippo^a, F. Ligabue^{a,c}, E. Manca^{a,c}, G. Mandorli^{a,c}, A. Messineo^{a,b}, F. Palla^a, A. Rizzi^{a,b}, G. Rolandi^{30}, P. Spagnolo^a, R. Tenchini^a, G. Tonelli^{a,b}, A. Venturi^a, P.G. Verdini^a

INFN Sezione di Roma ^{a}, Sapienza Università di Roma ^{b}, Rome, Italy
L. Barone^{a,b}, F. Cavallari^a, M. Cipriani^{a,b}, D. Del Re^{a,b}, E. Di Marco^{a,b}, M. Diemoz^a, S. Gelli^{a,b}, E. Longo^{a,b}, B. Marzocchi^{a,b}, P. Meridiani^a, G. Organtini^{a,b}, F. Pandolfi^a, R. Paramatti^{a,b}, F. Preiato^{a,b}, S. Rahatlou^{a,b}, C. Rovelli^a, F. Santanastasio^{a,b}

INFN Sezione di Torino ^{a}, Università di Torino ^{b}, Torino, Italy, Università del Piemonte Orientale ^{c}, Novara, Italy
N. Amapane^{a,b}, R. Arcidiacono^{a,c}, S. Argiro^{a,b}, M. Arneodo^{a,c}, N. Bartosik^a, R. Bellan^{a,b}, C. Biino^a, A. Cappati^{a,b}, N. Cartiglia^a, F. Cenna^{a,b}, S. Cometti^a, M. Costa^{a,b}, R. Covarelli^{a,b}, N. Demaria^a, B. Kiani^{a,b}, C. Mariotti^a, S. Maselli^a, E. Migliore^{a,b}, V. Monaco^{a,b}, E. Monteil^{a,b}, M. Monteno^a, M.M. Obertino^{a,b}, L. Pacher^{a,b}, N. Pastrone^a, M. Pelliccioni^a, G.L. Pinna Angioni^{a,b}, A. Romero^{a,b}, M. Ruspa^{a,c}, R. Sacchi^{a,b}, R. Salvatico^{a,b}, K. Shchelina^{a,b}, V. Sola^a, A. Solano^{a,b}, D. Soldi^{a,b}, A. Staiano^a

INFN Sezione di Trieste ^{a}, Università di Trieste ^{b}, Trieste, Italy
S. Belforte^a, V. Candelise^{a,b}, M. Casarsa^a, F. Cossutti^a, A. Da Rold^{a,b}, G. Della Ricca^{a,b}, F. Vazzoler^{a,b}, A. Zanetti^a

Kyungpook National University, Daegu, Korea
D.H. Kim, G.N. Kim, M.S. Kim, J. Lee, S. Lee, S.W. Lee, C.S. Moon, Y.D. Oh, S.I. Pak, S. Sekmen, D.C. Son, Y.C. Yang

Chonnam National University, Institute for Universe and Elementary Particles, Kwangju, Korea
H. Kim, D.H. Moon, G. Oh

Hanyang University, Seoul, Korea
B. Francois, J. Goh^{31}, T.J. Kim

Korea University, Seoul, Korea
S. Cho, S. Choi, Y. Go, D. Gyun, S. Ha, B. Hong, Y. Jo, K. Lee, K.S. Lee, S. Lee, J. Lim, S.K. Park, Y. Roh

Sejong University, Seoul, Korea
H.S. Kim

Seoul National University, Seoul, Korea
J. Almond, J. Kim, J.S. Kim, H. Lee, K. Lee, K. Nam, S.B. Oh, B.C. Radburn-Smith, S.h. Seo, U.K. Yang, H.D. Yoo, G.B. Yu

University of Seoul, Seoul, Korea
D. Jeon, H. Kim, J.H. Kim, J.S.H. Lee, I.C. Park

Sungkyunkwan University, Suwon, Korea
Y. Choi, C. Hwang, J. Lee, I. Yu

Vilnius University, Vilnius, Lithuania
V. Dudenas, A. Juodagalvis, J. Vaitkus

National Centre for Particle Physics, Universiti Malaya, Kuala Lumpur, Malaysia
I. Ahmed, Z.A. Ibrahim, M.A.B. Md Ali[32], F. Mohamad Idris[33], W.A.T. Wan Abdullah, M.N. Yusli, Z. Zolkapli

Universidad de Sonora (UNISON), Hermosillo, Mexico
J.F. Benitez, A. Castaneda Hernandez, J.A. Murillo Quijada

Centro de Investigacion y de Estudios Avanzados del IPN, Mexico City, Mexico
H. Castilla-Valdez, E. De La Cruz-Burelo, M.C. Duran-Osuna, I. Heredia-De La Cruz[34], R. Lopez-Fernandez, J. Mejia Guisao, R.I. Rabadan-Trejo, M. Ramirez-Garcia, G. Ramirez-Sanchez, R. Reyes-Almanza, A. Sanchez-Hernandez

Universidad Iberoamericana, Mexico City, Mexico
S. Carrillo Moreno, C. Oropeza Barrera, F. Vazquez Valencia

Benemerita Universidad Autonoma de Puebla, Puebla, Mexico
J. Eysermans, I. Pedraza, H.A. Salazar Ibarguen, C. Uribe Estrada

Universidad Autónoma de San Luis Potosí, San Luis Potosí, Mexico
A. Morelos Pineda

University of Auckland, Auckland, New Zealand
D. Krofcheck

University of Canterbury, Christchurch, New Zealand
S. Bheesette, P.H. Butler

National Centre for Physics, Quaid-I-Azam University, Islamabad, Pakistan
A. Ahmad, M. Ahmad, M.I. Asghar, Q. Hassan, H.R. Hoorani, A. Saddique, M.A. Shah, M. Shoaib, M. Waqas

National Centre for Nuclear Research, Swierk, Poland
H. Bialkowska, M. Bluj, B. Boimska, T. Frueboes, M. Górski, M. Kazana, M. Szleper, P. Traczyk, P. Zalewski

Institute of Experimental Physics, Faculty of Physics, University of Warsaw, Warsaw, Poland
K. Bunkowski, A. Byszuk[35], K. Doroba, A. Kalinowski, M. Konecki, J. Krolikowski, M. Misiura, M. Olszewski, A. Pyskir, M. Walczak

Laboratório de Instrumentação e Física Experimental de Partículas, Lisboa, Portugal
M. Araujo, P. Bargassa, C. Beirão Da Cruz E Silva, A. Di Francesco, P. Faccioli, B. Galinhas, M. Gallinaro, J. Hollar, N. Leonardo, J. Seixas, G. Strong, O. Toldaiev, J. Varela

Joint Institute for Nuclear Research, Dubna, Russia
S. Afanasiev, P. Bunin, M. Gavrilenko, I. Golutvin, I. Gorbunov, A. Kamenev, V. Karjavine, A. Lanev, A. Malakhov, V. Matveev[36,37], P. Moisenz, V. Palichik, V. Perelygin, S. Shmatov, S. Shulha, N. Skatchkov, V. Smirnov, N. Voytishin, A. Zarubin

Petersburg Nuclear Physics Institute, Gatchina (St. Petersburg), Russia
V. Golovtsov, Y. Ivanov, V. Kim[38], E. Kuznetsova[39], P. Levchenko, V. Murzin, V. Oreshkin, I. Smirnov, D. Sosnov, V. Sulimov, L. Uvarov, S. Vavilov, A. Vorobyev

Institute for Nuclear Research, Moscow, Russia
Yu. Andreev, A. Dermenev, S. Gninenko, N. Golubev, A. Karneyeu, M. Kirsanov, N. Krasnikov, A. Pashenkov, D. Tlisov, A. Toropin

Institute for Theoretical and Experimental Physics, Moscow, Russia
V. Epshteyn, V. Gavrilov, N. Lychkovskaya, V. Popov, I. Pozdnyakov, G. Safronov, A. Spiridonov, A. Stepennov, V. Stolin, M. Toms, E. Vlasov, A. Zhokin

Moscow Institute of Physics and Technology, Moscow, Russia
T. Aushev

National Research Nuclear University 'Moscow Engineering Physics Institute' (MEPhI), Moscow, Russia
M. Chadeeva[40], P. Parygin, D. Philippov, S. Polikarpov[40], E. Popova, V. Rusinov

P.N. Lebedev Physical Institute, Moscow, Russia
V. Andreev, M. Azarkin, I. Dremin[37], M. Kirakosyan, A. Terkulov

Skobeltsyn Institute of Nuclear Physics, Lomonosov Moscow State University, Moscow, Russia
A. Baskakov, A. Belyaev, E. Boos, V. Bunichev, M. Dubinin[41], L. Dudko, A. Ershov, V. Klyukhin, N. Korneeva, I. Lokhtin, I. Miagkov, S. Obraztsov, M. Perfilov, V. Savrin, P. Volkov

Novosibirsk State University (NSU), Novosibirsk, Russia
A. Barnyakov[42], V. Blinov[42], T. Dimova[42], L. Kardapoltsev[42], Y. Skovpen[42]

Institute for High Energy Physics of National Research Centre 'Kurchatov Institute', Protvino, Russia
I. Azhgirey, I. Bayshev, S. Bitioukov, D. Elumakhov, A. Godizov, V. Kachanov, A. Kalinin, D. Konstantinov, P. Mandrik, V. Petrov, R. Ryutin, S. Slabospitskii, A. Sobol, S. Troshin, N. Tyurin, A. Uzunian, A. Volkov

National Research Tomsk Polytechnic University, Tomsk, Russia
A. Babaev, S. Baidali, V. Okhotnikov

University of Belgrade, Faculty of Physics and Vinca Institute of Nuclear Sciences, Belgrade, Serbia
P. Adzic[43], P. Cirkovic, D. Devetak, M. Dordevic, J. Milosevic

Centro de Investigaciones Energéticas Medioambientales y Tecnológicas (CIEMAT), Madrid, Spain
J. Alcaraz Maestre, A. Álvarez Fernández, I. Bachiller, M. Barrio Luna, J.A. Brochero Cifuentes, M. Cerrada, N. Colino, B. De La Cruz, A. Delgado Peris, C. Fernandez Bedoya, J.P. Fernández Ramos, J. Flix, M.C. Fouz, O. Gonzalez Lopez, S. Goy Lopez, J.M. Hernandez, M.I. Josa, D. Moran, A. Pérez-Calero Yzquierdo, J. Puerta Pelayo, I. Redondo, L. Romero, M.S. Soares, A. Triossi

Universidad Autónoma de Madrid, Madrid, Spain
C. Albajar, J.F. de Trocóniz

Universidad de Oviedo, Oviedo, Spain
J. Cuevas, C. Erice, J. Fernandez Menendez, S. Folgueras, I. Gonzalez Caballero, J.R. González Fernández, E. Palencia Cortezon, V. Rodríguez Bouza, S. Sanchez Cruz, P. Vischia, J.M. Vizan Garcia

Instituto de Física de Cantabria (IFCA), CSIC-Universidad de Cantabria, Santander, Spain
I.J. Cabrillo, A. Calderon, B. Chazin Quero, J. Duarte Campderros, M. Fernandez, P.J. Fernández Manteca, A. García Alonso, J. Garcia-Ferrero, G. Gomez, A. Lopez Virto,

J. Marco, C. Martinez Rivero, P. Martinez Ruiz del Arbol, F. Matorras, J. Piedra Gomez, C. Prieels, T. Rodrigo, A. Ruiz-Jimeno, L. Scodellaro, N. Trevisani, I. Vila, R. Vilar Cortabitarte

University of Ruhuna, Department of Physics, Matara, Sri Lanka
N. Wickramage

CERN, European Organization for Nuclear Research, Geneva, Switzerland
D. Abbaneo, B. Akgun, E. Auffray, G. Auzinger, P. Baillon, A.H. Ball, D. Barney, J. Bendavid, M. Bianco, A. Bocci, C. Botta, E. Brondolin, T. Camporesi, M. Cepeda, G. Cerminara, E. Chapon, Y. Chen, G. Cucciati, D. d'Enterria, A. Dabrowski, N. Daci, V. Daponte, A. David, A. De Roeck, N. Deelen, M. Dobson, M. Dünser, N. Dupont, A. Elliott-Peisert, P. Everaerts, F. Fallavollita[44], D. Fasanella, G. Franzoni, J. Fulcher, W. Funk, D. Gigi, A. Gilbert, K. Gill, F. Glege, M. Gruchala, M. Guilbaud, D. Gulhan, J. Hegeman, C. Heidegger, V. Innocente, A. Jafari, P. Janot, O. Karacheban[19], J. Kieseler, A. Kornmayer, M. Krammer[1], C. Lange, P. Lecoq, C. Lourenço, L. Malgeri, M. Mannelli, F. Meijers, J.A. Merlin, S. Mersi, E. Meschi, P. Milenovic[45], F. Moortgat, M. Mulders, J. Ngadiuba, S. Nourbakhsh, S. Orfanelli, L. Orsini, F. Pantaleo[16], L. Pape, E. Perez, M. Peruzzi, A. Petrilli, G. Petrucciani, A. Pfeiffer, M. Pierini, F.M. Pitters, D. Rabady, A. Racz, T. Reis, M. Rovere, H. Sakulin, C. Schäfer, C. Schwick, M. Seidel, M. Selvaggi, A. Sharma, P. Silva, P. Sphicas[46], A. Stakia, J. Steggemann, D. Treille, A. Tsirou, V. Veckalns[47], M. Verzetti, W.D. Zeuner

Paul Scherrer Institut, Villigen, Switzerland
L. Caminada[48], K. Deiters, W. Erdmann, R. Horisberger, Q. Ingram, H.C. Kaestli, D. Kotlinski, U. Langenegger, T. Rohe, S.A. Wiederkehr

ETH Zurich - Institute for Particle Physics and Astrophysics (IPA), Zurich, Switzerland
M. Backhaus, L. Bäni, P. Berger, N. Chernyavskaya, G. Dissertori, M. Dittmar, M. Donegà, C. Dorfer, T.A. Gómez Espinosa, C. Grab, D. Hits, T. Klijnsma, W. Lustermann, R.A. Manzoni, M. Marionneau, M.T. Meinhard, F. Micheli, P. Musella, F. Nessi-Tedaldi, J. Pata, F. Pauss, G. Perrin, L. Perrozzi, S. Pigazzini, M. Quittnat, C. Reissel, D. Ruini, D.A. Sanz Becerra, M. Schönenberger, L. Shchutska, V.R. Tavolaro, K. Theofilatos, M.L. Vesterbacka Olsson, R. Wallny, D.H. Zhu

Universität Zürich, Zurich, Switzerland
T.K. Aarrestad, C. Amsler[49], D. Brzhechko, M.F. Canelli, A. De Cosa, R. Del Burgo, S. Donato, C. Galloni, T. Hreus, B. Kilminster, S. Leontsinis, I. Neutelings, G. Rauco, P. Robmann, D. Salerno, K. Schweiger, C. Seitz, Y. Takahashi, A. Zucchetta

National Central University, Chung-Li, Taiwan
T.H. Doan, R. Khurana, C.M. Kuo, W. Lin, A. Pozdnyakov, S.S. Yu

National Taiwan University (NTU), Taipei, Taiwan
P. Chang, Y. Chao, K.F. Chen, P.H. Chen, W.-S. Hou, Arun Kumar, Y.F. Liu, R.-S. Lu, E. Paganis, A. Psallidas, A. Steen

Chulalongkorn University, Faculty of Science, Department of Physics, Bangkok, Thailand
B. Asavapibhop, N. Srimanobhas, N. Suwonjandee

Çukurova University, Physics Department, Science and Art Faculty, Adana, Turkey
A. Bat, F. Boran, S. Cerci[50], S. Damarseckin, Z.S. Demiroglu, F. Dolek, C. Dozen, I. Dumanoglu, S. Girgis, G. Gokbulut, Y. Guler, E. Gurpinar, I. Hos[51], C. Isik, E.E. Kangal[52], O. Kara, A. Kayis Topaksu, U. Kiminsu, M. Oglakci, G. Onengut, K. Ozdemir[53], S. Ozturk[54], A. Polatoz, B. Tali[50], U.G. Tok, S. Turkcapar, I.S. Zorbakir, C. Zorbilmez

Middle East Technical University, Physics Department, Ankara, Turkey
B. Isildak[55], G. Karapinar[56], M. Yalvac, M. Zeyrek

Bogazici University, Istanbul, Turkey
I.O. Atakisi, E. Gülmez, M. Kaya[57], O. Kaya[58], S. Ozkorucuklu[59], S. Tekten, E.A. Yetkin[60]

Istanbul Technical University, Istanbul, Turkey
M.N. Agaras, A. Cakir, K. Cankocak, Y. Komurcu, S. Sen[61]

Institute for Scintillation Materials of National Academy of Science of Ukraine, Kharkov, Ukraine
B. Grynyov

National Scientific Center, Kharkov Institute of Physics and Technology, Kharkov, Ukraine
L. Levchuk

University of Bristol, Bristol, United Kingdom
F. Ball, J.J. Brooke, D. Burns, E. Clement, D. Cussans, O. Davignon, H. Flacher, J. Goldstein, G.P. Heath, H.F. Heath, L. Kreczko, D.M. Newbold[62], S. Paramesvaran, B. Penning, T. Sakuma, D. Smith, V.J. Smith, J. Taylor, A. Titterton

Rutherford Appleton Laboratory, Didcot, United Kingdom
K.W. Bell, A. Belyaev[63], C. Brew, R.M. Brown, D. Cieri, D.J.A. Cockerill, J.A. Coughlan, K. Harder, S. Harper, J. Linacre, E. Olaiya, D. Petyt, C.H. Shepherd-Themistocleous, A. Thea, I.R. Tomalin, T. Williams, W.J. Womersley

Imperial College, London, United Kingdom
R. Bainbridge, P. Bloch, J. Borg, S. Breeze, O. Buchmuller, A. Bundock, D. Colling, P. Dauncey, G. Davies, M. Della Negra, R. Di Maria, G. Hall, G. Iles, T. James, M. Komm, C. Laner, L. Lyons, A.-M. Magnan, S. Malik, A. Martelli, J. Nash[64], A. Nikitenko[7], V. Palladino, M. Pesaresi, D.M. Raymond, A. Richards, A. Rose, E. Scott, C. Seez, A. Shtipliyski, G. Singh, M. Stoye, T. Strebler, S. Summers, A. Tapper, K. Uchida, T. Virdee[16], N. Wardle, D. Winterbottom, J. Wright, S.C. Zenz

Brunel University, Uxbridge, United Kingdom
J.E. Cole, P.R. Hobson, A. Khan, P. Kyberd, C.K. Mackay, A. Morton, I.D. Reid, L. Teodorescu, S. Zahid

Baylor University, Waco, USA
K. Call, J. Dittmann, K. Hatakeyama, H. Liu, C. Madrid, B. McMaster, N. Pastika, C. Smith

Catholic University of America, Washington, DC, USA
R. Bartek, A. Dominguez

The University of Alabama, Tuscaloosa, USA
A. Buccilli, S.I. Cooper, C. Henderson, P. Rumerio, C. West

Boston University, Boston, USA
D. Arcaro, T. Bose, D. Gastler, D. Pinna, D. Rankin, C. Richardson, J. Rohlf, L. Sulak, D. Zou

Brown University, Providence, USA
G. Benelli, X. Coubez, D. Cutts, M. Hadley, J. Hakala, U. Heintz, J.M. Hogan[65], K.H.M. Kwok, E. Laird, G. Landsberg, J. Lee, Z. Mao, M. Narain, S. Sagir[66], R. Syarif, E. Usai, D. Yu

University of California, Davis, Davis, USA
R. Band, C. Brainerd, R. Breedon, D. Burns, M. Calderon De La Barca Sanchez, M. Chertok,

J. Conway, R. Conway, P.T. Cox, R. Erbacher, C. Flores, G. Funk, W. Ko, O. Kukral, R. Lander, M. Mulhearn, D. Pellett, J. Pilot, S. Shalhout, M. Shi, D. Stolp, D. Taylor, K. Tos, M. Tripathi, Z. Wang, F. Zhang

University of California, Los Angeles, USA
M. Bachtis, C. Bravo, R. Cousins, A. Dasgupta, A. Florent, J. Hauser, M. Ignatenko, N. Mccoll, S. Regnard, D. Saltzberg, C. Schnaible, V. Valuev

University of California, Riverside, Riverside, USA
E. Bouvier, K. Burt, R. Clare, J.W. Gary, S.M.A. Ghiasi Shirazi, G. Hanson, G. Karapostoli, E. Kennedy, F. Lacroix, O.R. Long, M. Olmedo Negrete, M.I. Paneva, W. Si, L. Wang, H. Wei, S. Wimpenny, B.R. Yates

University of California, San Diego, La Jolla, USA
J.G. Branson, P. Chang, S. Cittolin, M. Derdzinski, R. Gerosa, D. Gilbert, B. Hashemi, A. Holzner, D. Klein, G. Kole, V. Krutelyov, J. Letts, M. Masciovecchio, D. Olivito, S. Padhi, M. Pieri, M. Sani, V. Sharma, S. Simon, M. Tadel, A. Vartak, S. Wasserbaech[67], J. Wood, F. Würthwein, A. Yagil, G. Zevi Della Porta

University of California, Santa Barbara - Department of Physics, Santa Barbara, USA
N. Amin, R. Bhandari, C. Campagnari, M. Citron, V. Dutta, M. Franco Sevilla, L. Gouskos, R. Heller, J. Incandela, A. Ovcharova, H. Qu, J. Richman, D. Stuart, I. Suarez, S. Wang, J. Yoo

California Institute of Technology, Pasadena, USA
D. Anderson, A. Bornheim, J.M. Lawhorn, N. Lu, H.B. Newman, T.Q. Nguyen, M. Spiropulu, J.R. Vlimant, R. Wilkinson, S. Xie, Z. Zhang, R.Y. Zhu

Carnegie Mellon University, Pittsburgh, USA
M.B. Andrews, T. Ferguson, T. Mudholkar, M. Paulini, M. Sun, I. Vorobiev, M. Weinberg

University of Colorado Boulder, Boulder, USA
J.P. Cumalat, W.T. Ford, F. Jensen, A. Johnson, E. MacDonald, T. Mulholland, R. Patel, A. Perloff, K. Stenson, K.A. Ulmer, S.R. Wagner

Cornell University, Ithaca, USA
J. Alexander, J. Chaves, Y. Cheng, J. Chu, A. Datta, K. Mcdermott, N. Mirman, J.R. Patterson, D. Quach, A. Rinkevicius, A. Ryd, L. Skinnari, L. Soffi, S.M. Tan, Z. Tao, J. Thom, J. Tucker, P. Wittich, M. Zientek

Fermi National Accelerator Laboratory, Batavia, USA
S. Abdullin, M. Albrow, M. Alyari, G. Apollinari, A. Apresyan, A. Apyan, S. Banerjee, L.A.T. Bauerdick, A. Beretvas, J. Berryhill, P.C. Bhat, K. Burkett, J.N. Butler, A. Canepa, G.B. Cerati, H.W.K. Cheung, F. Chlebana, M. Cremonesi, J. Duarte, V.D. Elvira, J. Freeman, Z. Gecse, E. Gottschalk, L. Gray, D. Green, S. Grünendahl, O. Gutsche, J. Hanlon, R.M. Harris, S. Hasegawa, J. Hirschauer, Z. Hu, B. Jayatilaka, S. Jindariani, M. Johnson, U. Joshi, B. Klima, M.J. Kortelainen, B. Kreis, S. Lammel, D. Lincoln, R. Lipton, M. Liu, T. Liu, J. Lykken, K. Maeshima, J.M. Marraffino, D. Mason, P. McBride, P. Merkel, S. Mrenna, S. Nahn, V. O'Dell, K. Pedro, C. Pena, O. Prokofyev, G. Rakness, L. Ristori, A. Savoy-Navarro[68], B. Schneider, E. Sexton-Kennedy, A. Soha, W.J. Spalding, L. Spiegel, S. Stoynev, J. Strait, N. Strobbe, L. Taylor, S. Tkaczyk, N.V. Tran, L. Uplegger, E.W. Vaandering, C. Vernieri, M. Verzocchi, R. Vidal, M. Wang, H.A. Weber, A. Whitbeck

University of Florida, Gainesville, USA
D. Acosta, P. Avery, P. Bortignon, D. Bourilkov, A. Brinkerhoff, L. Cadamuro, A. Carnes,

D. Curry, R.D. Field, S.V. Gleyzer, B.M. Joshi, J. Konigsberg, A. Korytov, K.H. Lo, P. Ma, K. Matchev, H. Mei, G. Mitselmakher, D. Rosenzweig, K. Shi, D. Sperka, J. Wang, S. Wang, X. Zuo

Florida International University, Miami, USA
Y.R. Joshi, S. Linn

Florida State University, Tallahassee, USA
A. Ackert, T. Adams, A. Askew, S. Hagopian, V. Hagopian, K.F. Johnson, T. Kolberg, G. Martinez, T. Perry, H. Prosper, A. Saha, C. Schiber, R. Yohay

Florida Institute of Technology, Melbourne, USA
M.M. Baarmand, V. Bhopatkar, S. Colafranceschi, M. Hohlmann, D. Noonan, M. Rahmani, T. Roy, F. Yumiceva

University of Illinois at Chicago (UIC), Chicago, USA
M.R. Adams, L. Apanasevich, D. Berry, R.R. Betts, R. Cavanaugh, X. Chen, S. Dittmer, O. Evdokimov, C.E. Gerber, D.A. Hangal, D.J. Hofman, K. Jung, J. Kamin, C. Mills, I.D. Sandoval Gonzalez, M.B. Tonjes, H. Trauger, N. Varelas, H. Wang, X. Wang, Z. Wu, J. Zhang

The University of Iowa, Iowa City, USA
M. Alhusseini, B. Bilki[69], W. Clarida, K. Dilsiz[70], S. Durgut, R.P. Gandrajula, M. Haytmyradov, V. Khristenko, J.-P. Merlo, A. Mestvirishvili, A. Moeller, J. Nachtman, H. Ogul[71], Y. Onel, F. Ozok[72], A. Penzo, C. Snyder, E. Tiras, J. Wetzel

Johns Hopkins University, Baltimore, USA
B. Blumenfeld, A. Cocoros, N. Eminizer, D. Fehling, L. Feng, A.V. Gritsan, W.T. Hung, P. Maksimovic, J. Roskes, U. Sarica, M. Swartz, M. Xiao, C. You

The University of Kansas, Lawrence, USA
A. Al-bataineh, P. Baringer, A. Bean, S. Boren, J. Bowen, A. Bylinkin, J. Castle, S. Khalil, A. Kropivnitskaya, D. Majumder, W. Mcbrayer, M. Murray, C. Rogan, S. Sanders, E. Schmitz, J.D. Tapia Takaki, Q. Wang

Kansas State University, Manhattan, USA
S. Duric, A. Ivanov, K. Kaadze, D. Kim, Y. Maravin, D.R. Mendis, T. Mitchell, A. Modak, A. Mohammadi, L.K. Saini

Lawrence Livermore National Laboratory, Livermore, USA
F. Rebassoo, D. Wright

University of Maryland, College Park, USA
A. Baden, O. Baron, A. Belloni, S.C. Eno, Y. Feng, C. Ferraioli, N.J. Hadley, S. Jabeen, G.Y. Jeng, R.G. Kellogg, J. Kunkle, A.C. Mignerey, S. Nabili, F. Ricci-Tam, Y.H. Shin, A. Skuja, S.C. Tonwar, K. Wong

Massachusetts Institute of Technology, Cambridge, USA
D. Abercrombie, B. Allen, V. Azzolini, A. Baty, G. Bauer, R. Bi, S. Brandt, W. Busza, I.A. Cali, M. D'Alfonso, Z. Demiragli, G. Gomez Ceballos, M. Goncharov, P. Harris, D. Hsu, M. Hu, Y. Iiyama, G.M. Innocenti, M. Klute, D. Kovalskyi, Y.-J. Lee, P.D. Luckey, B. Maier, A.C. Marini, C. Mcginn, C. Mironov, S. Narayanan, X. Niu, C. Paus, C. Roland, G. Roland, Z. Shi, G.S.F. Stephans, K. Sumorok, K. Tatar, D. Velicanu, J. Wang, T.W. Wang, B. Wyslouch

University of Minnesota, Minneapolis, USA
A.C. Benvenuti[†], R.M. Chatterjee, A. Evans, P. Hansen, J. Hiltbrand, Sh. Jain, S. Kalafut, M. Krohn, Y. Kubota, Z. Lesko, J. Mans, N. Ruckstuhl, R. Rusack, M.A. Wadud

University of Mississippi, Oxford, USA
J.G. Acosta, S. Oliveros

University of Nebraska-Lincoln, Lincoln, USA
E. Avdeeva, K. Bloom, D.R. Claes, C. Fangmeier, F. Golf, R. Gonzalez Suarez, R. Kamalieddin, I. Kravchenko, J. Monroy, J.E. Siado, G.R. Snow, B. Stieger

State University of New York at Buffalo, Buffalo, USA
A. Godshalk, C. Harrington, I. Iashvili, A. Kharchilava, C. Mclean, D. Nguyen, A. Parker, S. Rappoccio, B. Roozbahani

Northeastern University, Boston, USA
G. Alverson, E. Barberis, C. Freer, Y. Haddad, A. Hortiangtham, D.M. Morse, T. Orimoto, R. Teixeira De Lima, T. Wamorkar, B. Wang, A. Wisecarver, D. Wood

Northwestern University, Evanston, USA
S. Bhattacharya, J. Bueghly, O. Charaf, K.A. Hahn, N. Mucia, N. Odell, M.H. Schmitt, K. Sung, M. Trovato, M. Velasco

University of Notre Dame, Notre Dame, USA
R. Bucci, N. Dev, M. Hildreth, K. Hurtado Anampa, C. Jessop, D.J. Karmgard, N. Kellams, K. Lannon, W. Li, N. Loukas, N. Marinelli, F. Meng, C. Mueller, Y. Musienko[36], M. Planer, A. Reinsvold, R. Ruchti, P. Siddireddy, G. Smith, S. Taroni, M. Wayne, A. Wightman, M. Wolf, A. Woodard

The Ohio State University, Columbus, USA
J. Alimena, L. Antonelli, B. Bylsma, L.S. Durkin, S. Flowers, B. Francis, C. Hill, W. Ji, T.Y. Ling, W. Luo, B.L. Winer

Princeton University, Princeton, USA
S. Cooperstein, P. Elmer, J. Hardenbrook, S. Higginbotham, A. Kalogeropoulos, D. Lange, M.T. Lucchini, J. Luo, D. Marlow, K. Mei, I. Ojalvo, J. Olsen, C. Palmer, P. Piroué, J. Salfeld-Nebgen, D. Stickland, C. Tully, Z. Wang

University of Puerto Rico, Mayaguez, USA
S. Malik, S. Norberg

Purdue University, West Lafayette, USA
A. Barker, V.E. Barnes, S. Das, L. Gutay, M. Jones, A.W. Jung, A. Khatiwada, B. Mahakud, D.H. Miller, N. Neumeister, C.C. Peng, S. Piperov, H. Qiu, J.F. Schulte, J. Sun, F. Wang, R. Xiao, W. Xie

Purdue University Northwest, Hammond, USA
T. Cheng, J. Dolen, N. Parashar

Rice University, Houston, USA
Z. Chen, K.M. Ecklund, S. Freed, F.J.M. Geurts, M. Kilpatrick, W. Li, B.P. Padley, R. Redjimi, J. Roberts, J. Rorie, W. Shi, Z. Tu, A. Zhang

University of Rochester, Rochester, USA
A. Bodek, P. de Barbaro, R. Demina, Y.t. Duh, J.L. Dulemba, C. Fallon, T. Ferbel, M. Galanti, A. Garcia-Bellido, J. Han, O. Hindrichs, A. Khukhunaishvili, E. Ranken, P. Tan, R. Taus

Rutgers, The State University of New Jersey, Piscataway, USA
A. Agapitos, J.P. Chou, Y. Gershtein, E. Halkiadakis, A. Hart, M. Heindl, E. Hughes, S. Kaplan, R. Kunnawalkam Elayavalli, S. Kyriacou, A. Lath, R. Montalvo, K. Nash, M. Osherson, H. Saka, S. Salur, S. Schnetzer, D. Sheffield, S. Somalwar, R. Stone, S. Thomas, P. Thomassen, M. Walker

University of Tennessee, Knoxville, USA
A.G. Delannoy, J. Heideman, G. Riley, S. Spanier

Texas A&M University, College Station, USA
O. Bouhali[73], A. Celik, M. Dalchenko, M. De Mattia, A. Delgado, S. Dildick, R. Eusebi, J. Gilmore, T. Huang, T. Kamon[74], S. Luo, R. Mueller, D. Overton, L. Perniè, D. Rathjens, A. Safonov

Texas Tech University, Lubbock, USA
N. Akchurin, J. Damgov, F. De Guio, P.R. Dudero, S. Kunori, K. Lamichhane, S.W. Lee, T. Mengke, S. Muthumuni, T. Peltola, S. Undleeb, I. Volobouev, Z. Wang

Vanderbilt University, Nashville, USA
S. Greene, A. Gurrola, R. Janjam, W. Johns, C. Maguire, A. Melo, H. Ni, K. Padeken, J.D. Ruiz Alvarez, P. Sheldon, S. Tuo, J. Velkovska, M. Verweij, Q. Xu

University of Virginia, Charlottesville, USA
M.W. Arenton, P. Barria, B. Cox, R. Hirosky, M. Joyce, A. Ledovskoy, H. Li, C. Neu, T. Sinthuprasith, Y. Wang, E. Wolfe, F. Xia

Wayne State University, Detroit, USA
R. Harr, P.E. Karchin, N. Poudyal, J. Sturdy, P. Thapa, S. Zaleski

University of Wisconsin - Madison, Madison, WI, USA
M. Brodski, J. Buchanan, C. Caillol, D. Carlsmith, S. Dasu, I. De Bruyn, L. Dodd, B. Gomber, M. Grothe, M. Herndon, A. Hervé, U. Hussain, P. Klabbers, A. Lanaro, K. Long, R. Loveless, T. Ruggles, A. Savin, V. Sharma, N. Smith, W.H. Smith, N. Woods

†: Deceased
1: Also at Vienna University of Technology, Vienna, Austria
2: Also at IRFU, CEA, Université Paris-Saclay, Gif-sur-Yvette, France
3: Also at Universidade Estadual de Campinas, Campinas, Brazil
4: Also at Federal University of Rio Grande do Sul, Porto Alegre, Brazil
5: Also at Université Libre de Bruxelles, Bruxelles, Belgium
6: Also at University of Chinese Academy of Sciences, Beijing, China
7: Also at Institute for Theoretical and Experimental Physics, Moscow, Russia
8: Also at Joint Institute for Nuclear Research, Dubna, Russia
9: Also at Cairo University, Cairo, Egypt
10: Also at Helwan University, Cairo, Egypt
11: Now at Zewail City of Science and Technology, Zewail, Egypt
12: Also at Department of Physics, King Abdulaziz University, Jeddah, Saudi Arabia
13: Also at Université de Haute Alsace, Mulhouse, France
14: Also at Skobeltsyn Institute of Nuclear Physics, Lomonosov Moscow State University, Moscow, Russia
15: Also at Tbilisi State University, Tbilisi, Georgia
16: Also at CERN, European Organization for Nuclear Research, Geneva, Switzerland
17: Also at RWTH Aachen University, III. Physikalisches Institut A, Aachen, Germany
18: Also at University of Hamburg, Hamburg, Germany

19: Also at Brandenburg University of Technology, Cottbus, Germany
20: Also at Institute of Physics, University of Debrecen, Debrecen, Hungary
21: Also at Institute of Nuclear Research ATOMKI, Debrecen, Hungary
22: Also at MTA-ELTE Lendület CMS Particle and Nuclear Physics Group, Eötvös Loránd University, Budapest, Hungary
23: Also at Indian Institute of Technology Bhubaneswar, Bhubaneswar, India
24: Also at Institute of Physics, Bhubaneswar, India
25: Also at Shoolini University, Solan, India
26: Also at University of Visva-Bharati, Santiniketan, India
27: Also at Isfahan University of Technology, Isfahan, Iran
28: Also at Plasma Physics Research Center, Science and Research Branch, Islamic Azad University, Tehran, Iran
29: Also at Università degli Studi di Siena, Siena, Italy
30: Also at Scuola Normale e Sezione dell'INFN, Pisa, Italy
31: Also at Kyunghee University, Seoul, Korea
32: Also at International Islamic University of Malaysia, Kuala Lumpur, Malaysia
33: Also at Malaysian Nuclear Agency, MOSTI, Kajang, Malaysia
34: Also at Consejo Nacional de Ciencia y Tecnología, Mexico City, Mexico
35: Also at Warsaw University of Technology, Institute of Electronic Systems, Warsaw, Poland
36: Also at Institute for Nuclear Research, Moscow, Russia
37: Now at National Research Nuclear University 'Moscow Engineering Physics Institute' (MEPhI), Moscow, Russia
38: Also at St. Petersburg State Polytechnical University, St. Petersburg, Russia
39: Also at University of Florida, Gainesville, USA
40: Also at P.N. Lebedev Physical Institute, Moscow, Russia
41: Also at California Institute of Technology, Pasadena, USA
42: Also at Budker Institute of Nuclear Physics, Novosibirsk, Russia
43: Also at Faculty of Physics, University of Belgrade, Belgrade, Serbia
44: Also at INFN Sezione di Pavia [a], Università di Pavia [b], Pavia, Italy
45: Also at University of Belgrade, Faculty of Physics and Vinca Institute of Nuclear Sciences, Belgrade, Serbia
46: Also at National and Kapodistrian University of Athens, Athens, Greece
47: Also at Riga Technical University, Riga, Latvia
48: Also at Universität Zürich, Zurich, Switzerland
49: Also at Stefan Meyer Institute for Subatomic Physics (SMI), Vienna, Austria
50: Also at Adiyaman University, Adiyaman, Turkey
51: Also at Istanbul Aydin University, Istanbul, Turkey
52: Also at Mersin University, Mersin, Turkey
53: Also at Piri Reis University, Istanbul, Turkey
54: Also at Gaziosmanpasa University, Tokat, Turkey
55: Also at Ozyegin University, Istanbul, Turkey
56: Also at Izmir Institute of Technology, Izmir, Turkey
57: Also at Marmara University, Istanbul, Turkey
58: Also at Kafkas University, Kars, Turkey
59: Also at Istanbul University, Faculty of Science, Istanbul, Turkey
60: Also at Istanbul Bilgi University, Istanbul, Turkey
61: Also at Hacettepe University, Ankara, Turkey
62: Also at Rutherford Appleton Laboratory, Didcot, United Kingdom
63: Also at School of Physics and Astronomy, University of Southampton, Southampton,

United Kingdom
64: Also at Monash University, Faculty of Science, Clayton, Australia
65: Also at Bethel University, St. Paul, USA
66: Also at Karamanoğlu Mehmetbey University, Karaman, Turkey
67: Also at Utah Valley University, Orem, USA
68: Also at Purdue University, West Lafayette, USA
69: Also at Beykent University, Istanbul, Turkey
70: Also at Bingol University, Bingol, Turkey
71: Also at Sinop University, Sinop, Turkey
72: Also at Mimar Sinan University, Istanbul, Istanbul, Turkey
73: Also at Texas A&M University at Qatar, Doha, Qatar
74: Also at Kyungpook National University, Daegu, Korea